Walport, F., Gardner, L., and Nethercot, D.A. (2020). Equivalent bow imperfections for use in design by second order inelastic analysis. *Structures*, 26: 670-685.

Equivalent bow imperfections for use in design by second order inelastic analysis

F. Walport, L. Gardner and D.A. Nethercot

Imperial College London, London, UK

E-mails: fiona.walport12@imperial.ac.uk, leroy.gardner@imperial.ac.uk,

d.nethercot@imperial.ac.uk

Abstract: *The stability of compression members is typically assessed through buckling curves, which include the influence of initial geometric imperfections and residual stresses. Alternatively, the capacity may be obtained more directly by carrying out either an elastic or an inelastic second order analysis using equivalent bow imperfections that account for both geometric imperfections and residual stresses. For design by second order elastic analysis, following the recommendations of EN 1993-1-1, the magnitudes of the equivalent bow imperfections can either be back-calculated for a given member to provide the same result as would be obtained from the member buckling curves or can be taken more simply as a fixed proportion of the member length. In both cases, a subsequent M–N (bending + axial) cross-section check is also required, which can be either linear elastic or linear plastic. For design by second order inelastic analysis, also referred to as design by geometrically and materially nonlinear analysis with imperfections (GMNIA) there are currently no suitable recommendations for the magnitudes of equivalent bow imperfections and, as demonstrated herein, it is not generally appropriate to use equivalent bow imperfections developed on the basis of elastic analysis. Equivalent bow imperfections suitable for use in design by second order inelastic analysis are therefore established in the present paper. The equivalent bow imperfections are calibrated against benchmark FE results, generated using geometrically and materially nonlinear analysis with geometric imperfections of L/1000 (L being the member*

length) and residual stresses. Based on the results obtained, an equivalent bow imperfection amplitude $e_0 = \alpha L/150$ (α being the traditional imperfection factor set out in EC3), is proposed for both steel and stainless steel elements and shown to yield accurate results. The reliability of the proposed approach is assessed, using the first order reliability method set out in EN 1990, against the benchmark FE ultimate loads, where it is shown that partial safety factors of 1.0 for steel and 1.1 for stainless steel can be adopted.

Keywords: Advanced analysis; Cold-formed steel; Equivalent imperfections; Flexural buckling; Global analysis; Inelastic analysis; Plastic design; Stainless steel; Steel

1. INTRODUCTION

Imperfections inevitably occur in practice in the manufacturing and fabrication of steel members and in the construction of structural systems. The load-carrying capacity of structural elements in compression is sensitive to imperfections; it is therefore essential that their deleterious influence be accounted for in design. Member imperfections include both initial geometric out-of-straightness and residual stresses. Depending on the adopted method of analysis and design, different magnitudes of initial imperfection are required in order to achieve a given load-carrying capacity. The appropriate choice of imperfection magnitude depends on: (i) the type of imperfection considered i.e. geometric imperfections only or equivalent imperfections accounting for both geometric out-of-straightness and residual stresses, (ii) the analysis type, (iii) the considered cross-section failure criterion and (iv) the benchmark resistance against which the choice of imperfection is assessed. EN 1090-2 [1] specifies manufacturing tolerances on member out-of-straightness and EN 1993-1-5 [2] recommends that 80% of the geometric manufacturing tolerance be applied as the geometric imperfection.

The stability of compression members is typically assessed through buckling curves, in which the effects of imperfections are incorporated. The European buckling curves [3], originally developed in [4–6], are based on the Perry–Robertson formulation and are underpinned by extensive test and numerical data; member resistances determined using the EN 1993-1-1 [3] buckling curves are therefore presupposed to be "correct" and have been taken as the target results in the development of imperfection rules for design by second order elastic analysis set out in EN 1993-1-1 and its upcoming revision prEN 1993-1-1 [7].

The use of buckling curves and member buckling checks can be avoided if member buckling can be directly captured in the structural analysis. To achieve this, a second order – also referred to as a geometrically nonlinear or advanced – analysis with appropriate member imperfections, is required. Member imperfections can be accounted for either through modelling the imperfect geometry or by applying a set of equivalent horizontal forces. Direct modelling of residual stresses in an analysis can present challenges to the designer; EN 1993-1-1 [3] therefore provides 'equivalent' bow imperfections that implicitly account for the combined effects of geometric and material (i.e. residual stresses) imperfections. These equivalent bow imperfections are for use with second order elastic analysis i.e. geometrically nonlinear analysis with imperfections (GNIA). There are no equivalent provisions for use with second order inelastic, or geometrically and materially nonlinear, analysis; this limitation is addressed herein.

Geometrically and materially nonlinear analysis with imperfections (GMNIA), incorporates material nonlinearity (plastic zone/fibre element model) as well as geometric nonlinearity in the analysis, and allows for accurate predictions of the full load–deformation response of a structure. Since the effects of loss of stiffness due to buckling and plasticity of the individual members within the structure are captured, a more accurate representation of the actual distribution of forces and moments, as compared to first order elastic analysis, is achieved.

Hence, both safer, more consistent and more efficient design can result from design by advanced inelastic analysis with imperfections or GMNIA. With improvements in computational power and software, design by GMNIA is becoming more widespread in practice and is receiving a growing level of attention in research [8–14]. Suitable equivalent bow imperfections for use in design by advanced inelastic analysis are therefore urgently needed. While significant capacity benefits are not expected from the use of second order inelastic analysis at the individual member level, the increased accuracy in capturing stiffness reductions and resulting deformations can lead to considerable benefits at the system level, both in terms of a more streamlined design process and structural safety and efficiency. Appropriate recommendations for both steel and stainless steel elements are made in the present paper.

2. EUROCODE 3 PROVISIONS FOR DESIGN BY SECOND ORDER ELASTIC ANALYSIS

In EN 1993-1-1 [3] and prEN 1993-1-1 [7], equivalent initial bow imperfection magnitudes e_0 for design by second order elastic analysis may be determined in two ways; (1) by back-calculating the required imperfection from the buckling curves or (2) by the use of approximate tabulated values. The tabulated approach [15,16] generally yields upper bound values of equivalent bow imperfections relative to the back-calculated values, resulting in safe-sided predictions of buckling resistance. The two approaches are described in more detail in the following sections.

2.1. Back-calculated equivalent bow imperfections

In EN 1993-1-1 and prEN 1993-1-1, Eq. (1) is provided for back-calculating equivalent bow imperfections e_0, where α is the imperfection factor for the relevant buckling curve, $\bar{\lambda}$ is the member slenderness, M_{Rk} is the characteristic moment resistance of the critical cross-section and N_{Rk} is the characteristic axial resistance of the critical cross-section. This equation was derived on the basis of a linear moment–axial (M–N) cross-section failure criterion, under axial load N and second order moment $M = Ne_0(1/(1-N/N_{\mathrm{cr}}))$, as described by Lindner et al. [15]. The calculation of e_0 depends on the column slenderness, which requires the determination of the effective buckling length of the member.

$$e_0 = \alpha\left(\bar{\lambda} - 0.2\right)\frac{M_{\mathrm{Rk}}}{N_{\mathrm{Rk}}} \quad \text{for} \quad \bar{\lambda} > 0.2 \tag{1}$$

Column buckling resistances determined using GNIA with the imperfection amplitude given by Eq. (1) are the same as those obtained from the European buckling curves. This is illustrated in Figure 1, which shows second order elastic force–moment paths for the critical mid-height cross-section of a column subjected to axial compression. If a linear elastic cross-section check is utilised, as given by Eq. (2), then $N_{\mathrm{Rk}} = N_{\mathrm{pl}}$, where N_{pl} is the axial cross-section resistance Af_y, with A being the cross-sectional area and f_y the material yield stress, and $M_{\mathrm{Rk}} = M_{\mathrm{el}}$ (i.e. the elastic moment capacity) and the back-calculated imperfection $e_{0,\mathrm{el,b\text{-}c}}$ results in a force–moment path that exactly intersects the linear elastic interaction surface at the buckling resistance of the column N_{EC3}.

$$\frac{N}{N_{\mathrm{pl}}} + \frac{M}{M_{\mathrm{el}}} = 1 \tag{2}$$

Similarly, if a linear plastic cross-section check is assumed, as given by Eq. (3), which is only permitted for Class 1 and 2 cross-sections, then $N_{\mathrm{Rk}} = N_{\mathrm{pl}}$ and $M_{\mathrm{Rk}} = M_{\mathrm{pl}}$ (i.e. the plastic moment capacity) and the back-calculated imperfection $e_{0,\mathrm{pl,b\text{-}c}}$ results in a force–moment path that

exactly intersects the linear plastic interaction surface at the buckling resistance of the column N_{EC3}.

$$\frac{N}{N_{pl}} + \frac{M}{M_{pl}} = 1 \tag{3}$$

The imperfection calculated using the linear plastic interaction surface $e_{0,pl,b\text{-}c}$ is larger than that calculated using the linear elastic interaction surface $e_{0,el,b\text{-}c}$ to compensate for the loss in stiffness due to the material nonlinearity that would occur in practice beyond the point of first yield, but is not captured in an elastic analysis. Note that utilising a nonlinear plastic cross-section check with Eq. (1) is not appropriate and will yield incorrect solutions due to the equation having been derived on the basis of a linear M–N interaction. For combined loading, the influence of the applied external moment should also be considered.

EN 1993-1-3 [17] and EN 1993-1-4 [18] give supplementary rules for the design of cold-formed steel and stainless steel structures, but currently provide no additional guidance for global analysis; consequently, the EN 1993-1-1 rules are assumed to apply. When an elastic second order analysis is used, the expressions for back-calculating equivalent bow imperfections are essentially equally applicable to both cold-formed steel and stainless steel design. However, the limiting slenderness $\bar{\lambda}_0$ in the stainless steel buckling curves is not a constant value (as is the case for hot-rolled and cold-formed steel), and hence a small modification is required – see Eq. (4). It is proposed that this modified equation be included in the upcoming revision to EN 1993-1-4.

$$e_0 = \alpha\left(\bar{\lambda} - \bar{\lambda}_0\right)\frac{M_{Rk}}{N_{Rk}} \quad \text{for} \quad \bar{\lambda} > \bar{\lambda}_0 \tag{4}$$

2.2. Tabulated equivalent bow imperfections

In addition to the method for back-calculating the required equivalent imperfection magnitude, prEN 1993-1-1 [7] provides tabulated values e_0/L, which are dependent on the cross-section type, axis of buckling and cross-section M-N failure criterion (linear elastic ($e_{0,el,tab}$) or linear plastic ($e_{0,pl,tab}$)). As shown in Figure 2, these imperfections are intended to approximate the back-calculated imperfections while remaining safe-sided and reducing the complexity of the calculation by avoiding the dependency on slenderness and, therefore, effective buckling lengths, which can be difficult to determine in practice [19].

The tabulated values e_0/L are determined using Eq. (5), where L is the member length, α is the imperfection factor for the associated column buckling curve and allows for the influence of residual stresses, ε accounts for the material strength and is defined by Eq. (6), where f_y is the yield stress in N/mm^2, and β is the reference relative bow imperfection that depends on the axis of buckling and the adopted cross-section failure criterion (linear elastic or linear plastic). These imperfections were developed by Lindner et al. [16], are included in prEN 1993-1-1 [7] and will replace those given in EN 1993-1-1. As for the back-calculated imperfections, it is not appropriate to utilise a nonlinear plastic cross-section check.

$$\frac{e_0}{L} = \frac{\alpha\beta}{\varepsilon} \tag{5}$$

$$\varepsilon = \sqrt{\frac{235}{f_y}} \tag{6}$$

For design by second order elastic analysis, these tabulated equivalent imperfections apply equally to cold-formed steel and stainless steel members, provided the appropriate value of α is employed (i.e. referring to EN 1993-1-4 for stainless steel). Note that the definition of ε given in EN 1993-1-4 [18] is due to be simplified to Eq. (6) in the upcoming version of the code.

3. DETERMINATION OF REQUIRED EQUIVALENT BOW IMPERFECTIONS FOR DESIGN BY SECOND ORDER INELASTIC ANALYSIS

3.1. Introduction and illustration of shortcomings in current provisions

The equivalent imperfections included in prEN 1993-1-1 [7] were derived on the basis of a second order elastic analysis and a linear M–N cross-section design check. Their use in design by second order elastic analysis gives the same result as the EN 1993-1-1 buckling curves if the back-calculated imperfection values are used, or a close, but safe-sided buckling resistance if the tabulated imperfection values are used. However, use of these imperfections, whether employing the back-calculated or tabulated values, in design by inelastic (plastic zone, distributed plasticity or fibre) analysis is not generally appropriate, and can give over-predictions (i.e. unconservative results) or under-predictions (i.e. conservative results) of buckling resistance depending on the form of the adopted material stress-strain curve. This is illustrated in Figures 3 and 4, respectively.

In Figure 3, the critical cross-section force–moment path obtained from a second order inelastic (plastic zone) analysis of a hot-rolled steel I-section column with an elastic, perfectly plastic material model (followed by strain hardening [20] though with no influence in this case) and a back-calculated imperfection magnitude using the linear elastic cross-section check is shown; major axis buckling is considered in Figure 3a and minor axis buckling is considered in Figure 3b. It may be seen that the peak load determined from the analysis is higher than the buckling resistance determined according to the EN 1993-1-1 buckling curves, with the over-prediction being more severe for minor axis buckling than for major axis buckling. This is because the

spread of plasticity through the cross-section after first yield and prior to the attainment of the peak load is more extensive about the minor axis, i.e. there is greater post first-yield capacity.

In Figure 4, the critical cross-section force–moment path obtained from a second order inelastic (plastic zone) analysis of a stainless steel I-section column with a nonlinear material stress–strain curve (see Section 3.3.2 [21,22]), and a back-calculated imperfection magnitude determined using the linear elastic cross-section check (i.e. $e_0 = e_{0,el,b\text{-}c}$), is shown. The nonlinear material model results in early yielding and a highly conservative peak load prediction in comparison with the resistance obtained from the Eurocode buckling curves $N_{EC3} = \chi N_{pl}$. From the comparisons shown in Figures 3 and 4, it is clear that equivalent imperfections derived on the basis of second order elastic analysis are not suitable for use in design by second order inelastic analysis.

Application of the existing Eurocode 3 equivalent imperfections in design by second order inelastic analysis has also been considered more widely across a range (see Section 3.3) of practical steel and stainless steel columns of different cross-section types (I-sections and square and rectangular hollow sections) and material grades (S235 to S690), with a focus around the critical member slenderness $\bar{\lambda} = 1$. The following overall observations can be made: use of the tabulated equivalent imperfections $e_{0,el,tab}$ given in prEN 1993-1-1 [7,15] in design by second order inelastic analysis results in over-predictions of resistance of up to 4% compared with the benchmark FE results (described in Section 3.3) and up to 7% compared with the Eurocode predictions for minor axis buckling of steel columns. If the back-calculated imperfections $e_{0,el,b\text{-}c}$ are utilised, then these errors increase to 8% on the unsafe side for both cases. On average, utilising $e_{0,el,tab}$ in design by GMNIA of steel columns buckling about the minor axis results in over-predictions of resistance of 2% compared with the benchmark FE results and 4% compared with the Eurocode buckling curves. In the case of stainless steel columns, owing to

the rounded stress–strain response, use of the back-calculated imperfections $e_{0,el,b\text{-}c}$ leads to under-predictions of major axis buckling resistance of up to 20% compared with the benchmark FE results. In all cases, utilising the prEN 1993-1-1 equivalent imperfections determined based on the plastic M–N interaction (i.e. $e_{0,pl,tab}$ or $e_{0,pl,b\text{-}c}$) in second order inelastic analysis results in highly conservative resistance predictions due to the effect of material nonlinearity being accounted for twice; for minor axis buckling of steel columns, resistance predictions are conservative by over 20% on average when utilising $e_{0,pl,tab}$ and by about 5% on average when utilising $e_{0,pl,b\text{-}c}$, compared with the benchmark FE predictions.

3.2. Choice of benchmark ultimate loads

To calculate the required equivalent imperfections for use in design by second order inelastic analysis, benchmark ultimate loads were sought. These were obtained from finite element models developed using beam elements with geometric imperfections in the form of a half-sine wave of amplitude $L/1000$ and residual stresses, as employed in the establishment of the EN 1993-1-1 buckling curves [5,6]. The use of benchmark FE results for the determination of suitable equivalent geometric imperfection amplitudes was favoured over the use of the existing buckling curves to avoid the unnecessary introduction of errors caused by fitting to results whose accuracy is restricted by the algebraic form of the underlying resistance function. This point is illustrated in Figures 5 and 6 for hot-rolled steel and stainless steel columns, respectively. Figure 5 shows normalised benchmark ultimate loads for hot-rolled I-sections of four different steel grades (S235, S355, S420 and S690), with a cross-section height-to-breadth (h/b) ratio greater than 1.2 and buckling about the major axis, plotted against member slenderness. The associated buckling curves (buckling curve a with $\alpha = 0.21$ for steel grades S235-S450 and buckling curve a_0 with $\alpha = 0.13$ for S460 steel and above) are also plotted in

the figure; it may be seen that buckling curve a becomes increasingly conservative with increasing steel grade relative to the benchmark FE results.

A similar shortcoming is shown in Figure 6 for the stainless steel buckling curves given in EN 1993-1-4, but this time in relation to changes in the strain hardening exponent n (see Section 3.3.2). Although in practice there are different values of n for different grades of stainless steel [18,21], the buckling curves are independent of n and therefore give no change in resistance when this parameter is varied; this is of course at odds with the real observed behaviour, as highlighted in Figure 6. Propagation of these systematic mismatches between the buckling curve and the benchmark FE data can be avoided by taking the benchmark FE results as the reference for establishing the equivalent imperfection amplitudes, and this is the approach taken herein.

3.3. Generation of benchmark data to underpin imperfection proposals for design by second order inelastic analysis

The calculation of ultimate loads from geometrically and materially nonlinear analysis with geometric imperfections and residual stresses is described in this section. These loads are taken as the benchmark loads against which the required equivalent bow imperfections, to reflect the combined effect of geometric imperfections and residual stresses, for use in design by second order inelastic analysis, are determined. Equivalent bow imperfection amplitudes are therefore sought such that the peaks of the force–moment curves obtained using a second order inelastic analysis with these imperfections align with the benchmark ultimate loads – see Figure 7.

3.3.1. Basic modelling assumptions

Finite element (FE) models were developed using the general purpose FE software ABAQUS [23]; the modelling approach has been extensively validated in previous studies [13,24–26]. Linear Timoshenko B31 beam elements, from the ABAQUS element library [23], were employed in all numerical simulations. Two cross-section shapes were considered – I-sections and square/rectangular hollow sections (SHS/RHS). Six I-section profiles (HEB 100, 200, 400, IPE 100, 140, HEM 200) and four hollow section profiles (RHS 200×100×10, 100×60×4, SHS 60×60×3, 60×60×2) were modelled, covering a range of cross-section height-to-breadth (h/b) ratios and cross-section slendernesses. The modelled members were pin ended, concentrically loaded and restrained against out-of-plane failure. A series of beam-columns was also considered in which the ratio of applied axial force to applied bending moment, as well as the shape of the bending moment diagram, were varied to investigate a range of scenarios. It was however the concentrically loaded members that showed the greatest sensitivity to imperfections and that controlled the determination of the required equivalent geometric imperfection amplitudes; comparisons between the proposals made herein and the benchmark beam-column FE results are nonetheless made in Section 4.1. A range of member lengths was modelled to give a range of slenderness values. For all FE models, a plastic zone analysis was carried out using the material parameters and stress–strain relationships described in Section 3.3.2, and the modified Riks method [23] was used to trace the full load–deformation response of the members.

3.3.2. Material modelling

Hot-rolled steel, cold-formed steel and stainless steel have distinctly different material stress–strain characteristics; hot-rolled steel is characterised by an elastic region with a clear yield point followed by a yield plateau and some strain hardening, whereas cold-formed steel and

stainless steel exhibit a more rounded stress–strain response with no clear yield point and continuous strain hardening. Appropriate descriptions of the stress–strain curves for all three materials are employed herein, as explained below and summarised in Table 1.

For hot-rolled steel, the quad-linear material model, developed by Yun and Gardner [20] and included in prEN 1993-1-14 [27], was utilised. Four steel grades were considered, with the key material properties listed in Table 1. For cold-formed steel and stainless steel, the stress–strain behaviour was described by the two-stage Ramberg–Osgood formulation [21,22,28,29], as given by Eq. (7) and (8), where ε and σ are the strain and stress respectively, f_y is the yield (0.2% proof) stress, E is the Young's modulus, f_u is the ultimate stress, E_y is the tangent modulus at the yield (0.2% proof) stress, defined by Eq. (9), $\varepsilon_{0.2}$ is the total strain at the 0.2% proof stress, equal to $0.002 + f_y/E$, ε_u is the ultimate strain, and n and m are the strain hardening exponents.

$$\varepsilon = \frac{\sigma}{E} + 0.002\left(\frac{\sigma}{f_y}\right)^n \quad \text{for} \quad \sigma \leq f_y \tag{7}$$

$$\varepsilon = \varepsilon_{0.2} + \frac{\sigma - f_y}{E_y} + \left(\varepsilon_u - \varepsilon_{0.2} - \frac{f_u - f_y}{E_y}\right)\left(\frac{\sigma - f_y}{f_u - f_y}\right)^m \quad \text{for} \quad f_y < \sigma \leq f_u \tag{8}$$

$$E_y = \frac{E}{1 + 0.002n\frac{E}{f_y}} \tag{9}$$

For cold-formed steel, grade S355 was considered and the values of the Ramberg–Osgood parameters were taken as those recommended by Gardner and Yun [22] and included in prEN 1993-1-14 [27]. For stainless steel, austenitic, duplex and ferritic grades were all considered, and the standardised material properties for numerical parametric studies of hot-rolled or welded sections defined by Afshan et al. [30] were employed, as summarised in Table 1. A

range of strain hardening exponents were considered to assess the influence of the degree of material nonlinearity [21,27].

3.3.3. Geometric imperfections and residual stresses

In the benchmark models, an initial bow imperfection was applied to the members in the form of a half-sine wave with a magnitude e_0 of 1/1000 of the member length L. Residual stress distributions differ in steel and stainless steel members due to the differences in physical and thermal properties [31]. For the steel I-section models, the ECCS [32] residual stress distribution for hot-rolled I-sections was employed, while for the stainless steel I-section models, the residual stress distribution for welded I-sections developed by Yuan et al. [33] was utilised, noting that stainless steel I-sections are predominantly produced by welding. The flanges and web of the cross-sections were each assigned 33 and 41 section points across their width for the steel [25] and stainless steel [34] members, respectively, to ensure that the corresponding residual stress distribution could be accurately captured. The residual stresses were introduced by defining the initial stress values at the section points through the SIGINI user subroutine [23]. Corresponding plastic strains were also assigned in the case of the stainless steel models [35]. Based on previous experimental and numerical findings [36–40], residual stresses were not included in the hollow section FE models – for hot-rolled hollow sections, their low magnitude results in minimal influence on buckling resistance, while for cold-formed hollow sections, the influence of the dominant through-thickness bending residual stresses is inherently captured in the nonlinear material stress–strain response [40].

3.4. Cross-section resistance

The distribution of internal forces and moments within a structure is influenced by the stiffnesses of the component members and the erosion thereof due to buckling and plasticity [41]. Design by second order inelastic analysis enables these effects to be captured directly and renders subsequent member buckling checks unnecessary. However, without the use of computationally expensive shell elements, cross-section checks and the associated allowance for local buckling remain necessary to avoid unattainable levels of spread of plasticity and plastic redistribution leading to overpredictions of structural resistance. This is important for all materials considered herein, but is of particular concern for those that exhibit a high degree of strain hardening, such as stainless steel. While these issues can be crudely overcome through the use of step-wise cross-section resistance checks, a considerably more rational, efficient and elegant solution is to apply strain limits [13,42]. The limiting strains are determined as a function of cross-section slenderness from the continuous strength method (CSM) base curve, as given by Eqs. (10) and (11) for hot-rolled steel design and Eqs. (12) and (13) for cold-formed steel and stainless steel design. Note that the different CSM base curve equations for hot-rolled steel and cold-formed/stainless steel design reflect the differences in the material stress–strain behaviour, which should be appropriately modelled in the inelastic analysis i.e. sharply defined yielding for hot-rolled steel [20] and a rounded response for cold-formed steel [22] and stainless steel [21].

$$\frac{\varepsilon_{\mathrm{csm}}}{\varepsilon_{\mathrm{y}}} = \frac{0.25}{\bar{\lambda}_{\mathrm{p}}^{3.6}} \quad \text{but} \quad \leq \Omega \quad \text{for} \quad \bar{\lambda}_{\mathrm{p}} \leq 0.68 \tag{10}$$

$$\frac{\varepsilon_{\mathrm{csm}}}{\varepsilon_{\mathrm{y}}} = \left(1 - \frac{0.222}{\bar{\lambda}_{\mathrm{p}}^{1.05}}\right) \frac{1}{\bar{\lambda}_{\mathrm{p}}^{1.05}} \quad \text{for} \quad \bar{\lambda}_{\mathrm{p}} > 0.68 \tag{11}$$

$$\frac{\varepsilon_{\mathrm{csm}}}{\varepsilon_{\mathrm{y}}} = \frac{0.25}{\bar{\lambda}_{\mathrm{p}}^{3.6}} + \frac{0.002}{\varepsilon_{\mathrm{y}}} \quad \text{but} \quad \leq \Omega \quad \text{for} \quad \bar{\lambda}_{\mathrm{p}} \leq 0.68 \tag{12}$$

$$\frac{\varepsilon_{csm}}{\varepsilon_y} = \left(1 - \frac{0.222}{\bar{\lambda}_p^{1.05}}\right) \frac{1}{\bar{\lambda}_p^{1.05}} + \frac{0.002\left(\sigma_{Ed,max}/f_y\right)^n}{\varepsilon_y} \quad \text{for} \quad \bar{\lambda}_p > 0.68 \tag{13}$$

In these equations, ε_{csm} is the maximum compressive strain that a cross-section can endure prior to failure, $\varepsilon_y = f_y/E$ (where E is the Young's modulus) is the yield strain, $\bar{\lambda}_p = \sqrt{f_y/\sigma_{cr}}$ is the local cross-sectional slenderness, with σ_{cr} being the elastic local buckling stress of the full cross-section [42,43], ε_u is the material ultimate tensile strain, $\sigma_{Ed,max}$ is the maximum stress level in the cross-section, n is the strain hardening exponent of the Ramberg–Osgood material model (see Section 3.3.2) and Ω is an upper bound multiple of the yield strain that can be applied on a project-by-project basis to reflect the level of plasticity that can be tolerated at the ultimate limit state, with a recommended value of 15.

3.5. Required equivalent bow imperfections for design by second order inelastic analysis

To calculate the required equivalent bow imperfections for use in design by second order inelastic analysis, FE models of the considered columns were run iteratively, varying the (equivalent) imperfection magnitude e_0 until the peak load coincided with the benchmark ultimate loads, calculated as described in Section 3.3, to within 1%, as illustrated in Figure 7.

Since the geometric imperfections alone have an amplitude of $L/1000$ in the benchmark FE models, the required values of the equivalent geometric imperfections $e_{0,req}$ will clearly be larger than this value to allow for influence of the residual stresses. Figure 8 shows the required $L/e_{0,req}$ values for an example austenitic stainless steel HEB 100 column with $\bar{\lambda} = 1$ and various n values. Residual stress patterns that exert compressive stresses at the flange tips have a more detrimental effect on minor axis buckling resistance than major axis buckling resistance, and this is reflected in the lower assigned buckling curve, with a higher imperfection factor α.

Incorporating the imperfection factor α in to the definition of $e_{0,req}$ captures this varying influence of the residual stresses.

The bow imperfections included in prEN 1993-1-1 [7] and given by Eq. (5) are a function of ε, to allow for the influence of material yield strength on the required imperfection amplitude for use in design by second order elastic analysis. With the influence of material yielding directly captured in the analysis, the required imperfection for inelastic analysis is no longer a function of ε. The varying influence of residual stresses for different cross-section types and axes of buckling can, as in Eq. (5), be captured through the imperfection factor α, as described above. Hence, introducing the reference relative bow imperfection β in a modified version of Eq. (5), the equivalent geometric imperfection for design by second order inelastic analysis is given by:

$$\frac{e_0}{L} = \alpha\beta \tag{14}$$

And the required values for the reference relative bow imperfection β_{req} can be determined from the required values of the equivalent bow imperfection $e_{0,req}$ using:

$$\beta_{req} = \frac{e_{0,\mathrm{req}}}{\alpha L} \tag{15}$$

In defining imperfections that are independent of the member slenderness $\bar{\lambda}$, to remove the complexity of calculating the effective length of a member or system, a level of conservatism must be accepted. This is highlighted in Figure 9 which shows required reference relative imperfection β_{req} values for an example hot-rolled steel I-section with varying member slenderness. The required reference relative imperfection values were at their maximum when $\bar{\lambda}$ = 3 for major axis buckling and $\bar{\lambda}$ = 0.5 for minor axis buckling. Only these critical slenderness values were therefore considered in the calculation of the required bow imperfections, resulting in conservative results for other values of slenderness. A similar

approach was adopted by Lindner et al. [15] in the derivation of equivalent geometric imperfections for design by second order elastic analysis. Note that cross-section checks were not critical in determining the buckling resistance of the considered columns by second order inelastic analysis, but do become critical in beam-columns, especially in the bending dominated scenarios.

The calculated required reference relative bow imperfection β_{req} values for 646 columns are plotted in Figure 10. Both major and minor axis buckling of the 6 I-section profiles described in Section 3.3.1 are considered, with the material stress–strain curves of hot-rolled steel and stainless steel given in Table 1. Hollow sections were not considered in the derivation of the required reference relative bow imperfection since the benchmark ultimate loads were determined with geometric imperfections only owing to the minimal influence of residual stresses, but are considered in Section 4.1 in the assessment of the resulting proposals.

3.6. Design recommendations

In this section, recommendations are made for equivalent bow imperfection magnitudes to be used in design by second order inelastic analysis of hot-rolled steel, cold-formed steel and stainless steel structural elements. The imperfection magnitudes may be applied either through direct modelling of the imperfection shape in the form of a half-sine wave along the member length or through the scaling of a suitable elastic critical buckling mode. Based on the required imperfections determined in Section 3.5 and shown in Figure 10, it is proposed to adopt a reference relative bow imperfection of $\beta = 1/150$ for use in design by second order inelastic analysis of columns and beam-columns, failing by in-plane flexural buckling about either axis, for all the materials and cross-sections examined herein. A single value was sought to provide accurate results for all cases while satisfying the reliability requirements, as assessed in Section

4. It can be seen in Figure 10, that there is little variation between the required imperfections between the two axes of buckling because the influence of cross-section shape and the spread of plasticity is captured in the inelastic analysis and the influence of residual stresses is captured through α. A value of β = 1/150 provides a safe sided approximation to almost all of the required reference relative bow imperfection β_{req} values; the suitability, application (through worked examples) and reliability of this proposal are demonstrated in the next section. Note that the magnitude of the equivalent bow imperfection e_0 should not be smaller than the magnitude of the geometric imperfection alone i.e. L/1000 – see limit in Eq. (21).

4. ASSESSMENT AND ILLUSTRATION OF DESIGN RECOMMENDATIONS

The reliability of the developed design recommendations i.e. design by second order inelastic analysis with equivalent bow imperfections determined from Eq. (14) with β= 1/150 and cross-section checks (both strength and strain based) as specified in Section 3.4, is assessed in this section with respect to the benchmark FE ultimate loads determined using GMNIA of columns and beam-columns with geometric imperfection amplitudes of L/1000 and residual stresses. Comparisons are also made against the results obtained using the conventional Eurocode design calculations. Application of the proposed design recommendations is demonstrated in Section 4.2 through a series of worked examples.

4.1. Reliability analysis

The reliability level and required partial safety factor γ_{M1} for use with the proposed equivalent bow imperfections in design by second order inelastic analysis are assessed using the first order reliability method (FORM) set out in EN 1990 [44] and further explained by Afshan et al. [45]. In EN 1990, for buildings, the target reliability index β is 3.8, corresponding to an overall target failure probability of 10^{-6} per year over a 50 year design life, and is adopted as the basis for the

derivation of the partial safety factors. The recommended values for the partial safety factor γ_{M1} are 1.0 for steel in EN 1993-1-1 and 1.1 for stainless steel in EN 1993-1-4. These are taken as the target values in the present study.

The adopted values of the mean-to-nominal yield strength ratio $f_{y,mean}/f_{y,norm}$ (i.e. the material over-strength) and the COV of the yield strength V_{fy} and geometric properties V_A were specified in accordance with prEN 1993-1-1 [7] for steel and Afshan et al. [45] for stainless steel. The COV of the Young's modulus V_E was taken equal to 0.03 for both materials [7]. The dependency of the column buckling resistance on the basic variables – yield stress f_y, cross-sectional area A and Young's modulus E changes with the member proportions and therefore between each numerical simulation. Hence, for each FE result, the dependency of the resistance, presented as the exponent (c, d and e) to which each basic variable should be raised, on f_y, A and E was determined using Eqs. (16), (17) and (18), respectively, where $N_{1.05fy}$ is the buckling load calculated from a numerical analysis with the yield stress multiplied by 1.05, $N_{1.05A}$ is the buckling load calculated from a numerical analysis with the cross-sectional area multiplied by 1.05, $N_{1.05E}$ is the buckling load calculated from a numerical analysis with the Young's modulus multiplied by 1.05 and N_{fy}, N_A and N_E represent the original buckling load with no alterations to yield stress, area or Young's modulus.

$$c = \frac{\ln\left(N_{1.05f_y}/N_{f_y}\right)}{\ln\left(1.05f_y/f_y\right)} \tag{16}$$

$$d = \frac{\ln(N_{1.05A}/N_A)}{\ln(1.05A/A)} \tag{17}$$

$$e = \frac{\ln(N_{1.05E}/N_E)}{\ln(1.05E/E)} \tag{18}$$

Figure 11 shows the determined values of the exponents c and d for all compression cases considered. As slenderness increases, the dependency on the yield stress f_y, and hence the

exponent c, reduces while the dependency on the cross-sectional area A, and hence the exponent d, increases. This is because the buckling load approaches the elastic buckling load as slenderness increases, which is a function of section geometry but independent of the yield stress f_y. The scatter in the results arises due to the differences in material characteristics and geometries across the range of results considered; for any individual case, the results follow a consistent path, as shown in Figure 12 for a hot-rolled S235 steel HEB 100 column buckling about the major axis. The varying influence of Young's modulus on the buckling resistance [46] is considered through the exponent e, the determined values for which are shown in Figure 13 for all compression cases considered. For low member slenderness, the member resistance is essentially the plastic squash load and the dependency on E, as captured through the value of the exponent e, approaches zero; in contrast, for high member slenderness, the buckling resistance tends towards the elastic buckling load and e tends towards unity. By calculating the exponent values for each numerical result, the varying degree of influence of the variables f_y, A and E on the load carrying capacity was incorporated into a combined coefficient of variation V_{rt}, given by Eq. (19) [47].

$$V_{rt} = \sqrt{\left(cV_{fy}\right)^2 + (dV_A)^2 + (eV_E)^2} \tag{19}$$

Note that although the use of the mean value of the Young's modulus E = 210,000 N/mm^2 is appropriate in the resistance functions set out in EN 1993-1-1 since the partial safety factors have been calibrated on the basis of this reference value, it is not, in the view of the authors, suitable for use in design by GMNIA (i.e. design by second order inelastic analysis). Consider, for example, a very slender column whose failure load will be close to the Euler load - using the mean value of E in a GMNIA, in conjunction with a partial safety factor of unity, results in the design value of the resistance being approximately equal to the mean value. Clearly, this does not satisfy the reliability requirements of EN 1990. To resolve this, it is proposed that the

characteristic value of E (i.e. the fifth percentile) is employed in design by GMNIA; this is somewhat equivalent to the use of the nominal value of f_y (rather than the mean value). The characteristic value of E is given in Annex E of prEN 1993-1-1 [7] as 200,000 N/mm^2, and this value has been used in the GMNIA design calculations performed in this paper. Likewise, a characteristic (fifth percentile) value of E for stainless steel has been calculated as 191,000 N/mm^2 and implemented in the GMNIA design calculations.

A summary of the results from the statistical analysis are included in Tables 2 to 5. Tables 2 and 3 present an assessment of the proposed approach against the benchmark results generated in Section 3.3 for I-section and hollow section columns, respectively. The assessment was carried out on 1464 columns (306 hot-rolled steel, 36 cold-formed steel and 1122 stainless steel), considering both major and minor axis buckling and six slenderness values ($\bar{\lambda}$ = 0.5, 1.0, 1.5, 2.0, 2.5, 3.0). A summary of the statistical analysis of the proposed approach applied to I-section and hollow section members under combined compression and bending about both the major and minor axes is presented in Tables 4 and 5, respectively. The assessment was carried out on 584 beam-columns (316 hot-rolled steel, 52 cold-formed steel and 216 stainless steel), considering both major and minor axis buckling, three slenderness values ($\bar{\lambda}$ = 0.5, 1.0, 1.5), four ratios of applied compression to bending and three bending moment distributions along the member length (ψ = 1.0, 0, −0.5), achieved by changing the ratio of applied end moments $\psi = M_2/M_1$. The partial safety factor for each case, as well as the mean correction factor b, the coefficient of variation of the proposed results relative to the benchmark results V_δ and the combined coefficient of variation incorporating the model and basic variable uncertainties V_r are presented in Tables 2 to 5. The mean correction factor b was calculated using a modified definition to that given in EN 1990 [44], based on the average ratio of benchmark resistance r_e to predicted resistance r_t, as given by Eq. (20), to avoid the derived value of b being biased towards the data points with higher absolute resistance values [47,48].

$$b = \frac{1}{n}\sum_{i=1}^{n}\frac{r_{\mathrm{e,i}}}{r_{\mathrm{t,i}}} \tag{20}$$

From Tables 2 to 5, it can be seen that the mean predictions are safe-sided (i.e. $b > 1.0$) and that the required partial factors γ_{M1} for design by second order inelastic analysis using the proposed imperfections are generally less than or equal to the recommended values of 1.0 for steel [3] and 1.1 for stainless steel [18], demonstrating that the proposals can be safely adopted in conjunction with these partial factors. The required γ_{M1} values for the steel members are slightly in excess of the target value of 1.0 but remain in line with the recommendations of the project SAFEBRICTILE [49,50], which also considers the influence of the coefficient of variation V_r, and deems a small exceedance of the target value to be acceptable. However, for the high strength steel hollow sections, the results indicate that a higher partial safety factor than that currently recommended is required; this arises due to the combination of a relatively low over-strength factor for high strength steel and the use of the highest buckling curve – buckling curve a_0. It is recommended that the use of buckling curve a_0 be reconsidered for high strength steel tubular sections; a similar recommendation was made by Wang and Gardner [51] upon assessment of the buckling curve against test and FE results on high strength steel hollow section columns. Using buckling curve a results in a safe-sided mean prediction, with $b = 1.02$. In the case of beam-columns, as bending increases the influence of geometric imperfections becomes increasingly insignificant and this is reflected in the b values being closer to unity in Tables 4 and 5 compared with Tables 2 and 3. The stainless steel buckling resistance predictions are generally more conservative than the steel results, particularly for the austenitic grades, and the required values of γ_{M1} are all less than the target value of 1.1.

The resistances obtained using the proposed approach N_{prop} are also compared with those determined using the conventional Eurocode member capacity checks N_{EC3}. For steel columns,

mean N_{EC3}/N_{prop} ratios close to unity are obtained (1.00 and 0.96 for S235 and S420 I -section columns, respectively, and 0.99 and 0.97 for S235 and S420 SHS and RHS columns, respectively). For stainless steel columns, the proposed approach generally yields conservative results relative to EN 1993-1-4, with the mean N_{EC3}/N_{prop} ratios being 1.08, 0.99 and 1.01 for austenitic, duplex and ferritic stainless steel I-section columns, respectively, and 1.11, 1.04 and 1.01 for austenitic, duplex and ferritic stainless steel SHS and RHS columns, respectively. As discussed in Section 3.2, the individual Eurocode buckling curves do not account for variation in material stress–strain properties and become increasingly conservative with increasing material grade compared with the benchmark FE strength predictions determined using a geometric imperfection of $L/1000$ and residual stresses, which a designer could directly employ. The slightly low average N_{EC3}/N_{prop} ratio of 0.96 for S420 I-sections is therefore deemed acceptable. This point is emphasised in Figures 14 a-c, which show normalised flexural buckling capacities against member slenderness. For each material grade, the buckling capacities using the proposed equivalent bow imperfections made herein N_{prop} are compared against both the benchmark ultimate loads N_{FE}, calculated as described in Section 3.3, and the Eurocode predictions N_{EC3}. The N_{FE}/N_{prop} values are consistently above unity, confirming the safe-sided nature of the predictions. However, relative to the capacity predictions obtained using the EC3 buckling curves N_{EC3}, the N_{prop} values become higher with increasing steel grade, reflecting not unconservative capacity predictions from the proposed method, but shortcomings in the EC3 buckling curves i.e. failure to predict higher normalised capacities with increasing steel grade for a given buckling curve.

4.2. Worked examples

Two worked examples are provided in this section to demonstrate the application of the proposed equivalent bow imperfections in design by second order inelastic analysis, as well as

the benefits compared with the current provisions. Figures 15 and 16 present worked examples for hot-rolled S235 steel and austenitic stainless steel (with f_y = 280 N/mm^2) members, respectively. Example 1 considers an HEB 100 column of member slenderness $\bar{\lambda}$ = 1.5 buckling about the major axis. The column has a local slenderness $\bar{\lambda}_p$ = 0.27 and a CSM strain limit $\varepsilon_{csm}/\varepsilon_y$ = 15 (when Ω = 15); since the failure is stability governed, the peak load factor is reached prior to the CSM strain limit. Example 2 considers a SHS 100×100×4 beam-column of member slenderness $\bar{\lambda}$ = 0.5 with a bending moment distribution of $\psi(=M_1/M_2)$ = 0 and an applied axial load and bending moment of $0.1N_{pl}$ and $0.9M_{pl}$, respectively. The beam-column has a local slenderness $\bar{\lambda}_p$ = 0.42 and a CSM strain limit $\varepsilon_{csm}/\varepsilon_y$ = 7.21. Load–displacement paths are plotted in Figures 15 and 16, as well as the resulting ultimate load predictions for each imperfection considered; a summary of the results for both examples is presented in Table 6. Benchmark ultimate loads N_{FE} are generated from geometrically and materially nonlinear analysis with geometric imperfections of L/1000 and residual stresses and the CSM strain limit applied, as outlined in Section 3.4.

Use of the proposed equivalent bow imperfections in design by second order inelastic analysis results in close but safe-sided capacity predictions compared with the benchmark FE results in both examples. Relative to design by second order elastic analysis using the prEN 1993-1-1 tabulated equivalent imperfections $e_{0,pl,tab}$ corresponding to a plastic M-N cross-section check, capacity predictions determined using the proposed approach (second order plastic zone analysis with $e_{0,prop}$ and applying the CSM strain limit) are 13% and 19% higher for examples 1 and 2, respectively. It can be seen in worked example 2 that limiting the cross-section resistance using the CSM strain limit results in significantly more accurate predictions than using the M-N cross-section check. Also, in this example, the imperfection magnitude has only a small effect on the member capacity since the member deformations are dominated by the applied bending – see the load–deformation paths in Figure 16.

4.3. Summary of recommendations

For design by second order elastic analysis, the tabulated equivalent bow imperfections set out in prEN 1993-1-1 [7] for steel design are equally applicable to stainless steel and cold-formed steel design. The stainless steel design rules include buckling curves with a varying limiting slenderness $\bar{\lambda}_0$ and therefore it is proposed that the modified back-calculated imperfection equation, given by Eq. (4) is included in the upcoming revision to EN 1993-1-4. Use of these existing imperfections (those determined for a linear plastic cross-section check) in second order plastic hinge analysis is also considered to be acceptable. However, for design by second order inelastic (plastic zone, distributed plasticity or fibre) analysis, use of these existing imperfections is not generally appropriate, and new equivalent bow imperfections, to account for the combined effects of geometric imperfections and residual stresses, have been derived, as given by Eq. (21), where α is the imperfection factor for the relevant buckling curve, as prescribed in EN 1993-1-1 and EN 1993-1-4. These imperfection magnitudes may be applied either through direct modelling of the imperfection shape as a half-sine wave or through the scaling of a suitable elastic critical buckling mode.

$$\frac{e_0}{L} = \alpha\beta = \frac{\alpha}{150} \quad \text{but} \quad \frac{e_0}{L} \geq \frac{1}{1000} \tag{21}$$

A reference relative bow imperfection $\beta = 1/150$ is proposed for all considered grades of steel and stainless steel and cross-section types, and has been shown to yield accurate and consistent results, though for high strength steel, it is recommended that the use of buckling curve a_0 be reconsidered, due to the low material over-strength. It is also proposed that the characteristic (i.e. the fifth percentile) value of E (i.e. E = 200,000 N/mm^2 for steel and E = 191,000 N/mm^2 for stainless steel) is employed in design by GMNIA to satisfy the reliability requirements of EN 1990.

It should also be verified that the cross-sectional resistance of the member, which relates to its local slenderness, is not exceeded either through the conduct of cross-section capacity checks or the application of strain limits, as described in Section 3.4 and illustrated in the examples set out in Section 4.2.

5. CONCLUSIONS

prEN 1993-1-1 provides equivalent bow imperfections that account for the combined effects of geometric imperfections and residual stresses for use in design by second order elastic analysis. If the back-calculated values are used, the resulting capacity is the same as that achieved using the buckling curves, while close, but safe-sided buckling resistances are obtained if the simplified tabulated values are used. While these imperfections are appropriate for use in design by second order elastic analysis, their use in design by second order inelastic analysis is not generally appropriate, and can lead to both unsafe and overly-conservative resistance predictions depending in particular on the shape and material properties of the examined cross-sections. Thus, new equivalent geometric imperfections suitable for use in design by second order inelastic (plastic zone, distributed plasticity and fibre) analysis were sought. Following calibration against benchmark FE ultimate loads generated using geometrically and materially nonlinear analysis with geometric imperfections of $L/1000$ and appropriate residual stresses, an equivalent bow imperfection amplitude $e_0 = \alpha\beta L$ was proposed. The varying influence of residual stresses for different cross-sections and axes of buckling is captured through the imperfection factor α, which is determined according to the buckling curves prescribed in EN 1993-1-1 and EN 1993-1-4 for steel and stainless steel, respectively. A value for the reference relative bow imperfection $\beta = 1/150$ was found to be suitable for all cases considered.

The reliability of the proposed approach was assessed against the benchmark FE ultimate loads, where it was shown that partial safety factors of 1.0 for steel and 1.1 for stainless steel could be adopted. The proposed equivalent bow imperfections for use in design by second order inelastic analysis consider the combined effects of geometrical imperfections and residual stresses and provide accurate resistance predictions while remaining simple and practical for application in structural design.

ACKNOWLEDGEMENTS

Funding for this investigation was received from the Imperial College PhD Scholarship scheme.

REFERENCES

[1] EN 1090-2. 2018. EN 1090-2 - Execution of steel structures and aluminium structures. Part 2: Technical requirements for steel structures. BSI; 2018.

[2] EN 1993-1-5. 2009. Eurocode 3 - Design of steel structures - Part 1-5 : Plated structural elements. Brussels: CEN; 2009.

[3] EN 1993-1-1. 2005. Eurocode 3: Design of steel structures - Part 1-1: General rules and rules for buildings. Brussels: CEN; 2005.

[4] Rondal, J., & Maquoi, R. 1979. Single equation for SSRC column strength curves. *Journal of the Structural Division (ASCE)*, 105: 247–50.

[5] Maquoi, R., & Rondal, J. 1978. Mise En Equation Des Nouvelles Courbes Europeennes De Flambement. *Construction Metallique*, 1: 17–30.

[6] Beer, H., & Schulz, G. 1970. Bases theoriques des courbes europeennes de flambement. *Construction Metallique*, 3: 37–56.

[7] prEN 1993-1-1. 2019. Eurocode 3 – Design of steel structures – Part 1-1: General rules and rules for buildings. 2019.

[8] Ziemian, R.D. 1990. Advanced methods of inelastic anlaysis in the limit states design of steel structures. Cornell University, 1990.

[9] Ziemian, R.D., McGuire, W., & Deierlein, G. 1992. Inelastic limit states design. Part 1: Planar frame studies. *Journal of Structural Engineering ASCE*, 118: 2532–49.

[10] Chan, S.L., & Chen, W.F. 2005. Advanced analysis as a new dimension for structural steel design. *Advanced Steel Construction*, 1: 87–102.

[11] Buonopane, S.G., & Schafer, B.W. 2006. Reliability of steel frames designed with advanced analysis. *Journal of Structural Engineering*, 132: 267–76.

[12] Zhang, H., Shayan, S., Rasmussen, K.J.R., & Ellingwood, B.R. 2016. System-based design of planar steel frames, I: Reliability framework. *Journal of Constructional Steel Research*, 123: 135–43.

[13] Fieber, A., Gardner, L., & Macorini, L. 2019. Design of structural steel members by advanced inelastic analysis with strain limits. *Engineering Structures*, 199: 109624.

[14] Gardner, L., Yun, X., Fieber, A., & Macorini, L. 2019. Steel design by advanced analysis: material modeling and strain limits. *Engineering*, 5: 243–9.

[15] Lindner, J., Kuhlmann, U., & Just, A. 2016. Verification of flexural buckling according to Eurocode 3 part 1-1 using bow imperfections. *Steel Construction*, 9: 349–62.

[16] Lindner, J., Kuhlmann, U., & Jörg, F. 2018. Initial bow imperfections e_0 for the verification of flexural buckling according to Eurocode 3 Part 1-1 – additional

considerations. *Steel Construction*, 11: 30–41.

[17] EN 1993-1-3. 2006. Eurocode 3 – Design of steel structures – Part 1-3: General rules - Supplementary rules for cold-formed members and sheeting. 2006.

[18] EN 1993-1-4:2006 + A1: 2015. Eurocode 3 - Design of steel structures - Part 1-4: General rules - Supplementary rules for stainless steels. Brussels: CEN; 2015.

[19] Liew, R.J.Y., White, D.W., & Chen, W.F. 1991. Beam-column design in steel frameworks- insights on current methods and trends. *Journal of Constructional Steel Research*, 18: 269–308.

[20] Yun, X., & Gardner, L. 2017. Stress-strain curves for hot-rolled steels. *Journal of Constructional Steel Research*, 133: 36–46.

[21] Arrayago, I., Real, E., & Gardner, L. 2015. Description of stress-strain curves for stainless steel alloys. *Materials and Design*, 87: 540–52.

[22] Gardner, L., & Yun, X. 2018. Description of stress-strain curves for cold-formed steels. *Construction and Building Materials*, 189: 527–38.

[23] ABAQUS. 2014. Abaqus CAE User's Manual, Version 6.14. Pawtucket, USA: Hibbitt, Karlsson & Sorensen, Inc.; 2014.

[24] Sena Cardoso, F., & Rasmussen, K.J.R. 2016. Finite element (FE) modelling of storage rack frames. *Journal of Constructional Steel Research*, 126: 1–14.

[25] Kucukler, M., Gardner, L., & Macorini, L. 2016. Development and assessment of a practical stiffness reduction method for the in-plane design of steel frames. *Journal of Constructional Steel Research*, 126: 187–200.

[26] Fieber, A., Gardner, L., & Macorini, L. 2020. Structural steel design using second-order inelastic analysis with strain limits. *Journal of Constructional Steel Research*, 168:

105980.

[27] prEN 1993-1-14. 2019. Eurocode 3 – Design of steel structures – Part 1-14: Design by FE analysis. 2019.

[28] Mirambell, E., & Real, E. 2000. On the calculation of deflections in structural stainless steel beams: an experimental and numerical investigation. *Journal of Constructional Steel Research*, 54: 109–33.

[29] Rasmussen, K.J.R. 2003. Full-range stress–strain curves for stainless steel alloys. *Journal of Constructional Steel Research*, 59: 47–61.

[30] Afshan, S., Zhao, O., & Gardner, L. 2019. Standardised material properties for numerical parametric studies of stainless steel structures and buckling curves for tubular columns. *Journal of Constructional Steel Research*, 152: 2–11.

[31] Gardner, L., & Ng, K.T. 2006. Temperature development in structural stainless steel sections exposed to fire. *Fire Safety Journal*, 41: 185–203.

[32] ECCS. 1984. Ultimate limit state calculations of sway frames with rigid joints. *No 33, Technical Committee 8 of the European Convention for Constructional Steelwork (ECCS)*, 1984.

[33] Yuan, H.X., Wang, Y.Q., Shi, Y.J., & Gardner, L. 2014. Residual stress distributions in welded stainless steel sections. *Thin-Walled Structures*, 79: 38–51.

[34] Walport, F., Gardner, L., Real, E., Arrayago, I., & Nethercot, D.A. 2019. Effects of material nonlinearity on the global analysis and stability of stainless steel frames. *Journal of Constructional Steel Research*, 152: 173–82.

[35] Kucukler, M., Xing, Z., & Gardner, L. 2020. Behaviour and design of stainless steel I-section columns in fire. *Journal of Constructional Steel Research*, 164: 105890.

[36] Gardner, L., & Nethercot, D.A. 2004. Numerical modeling of stainless steel structural components — A consistent approach. *Journal of Structural Engineering, ASCE*, 130: 1586–601.

[37] Ellobody, E., & Young, B. 2005. Structural performance of cold-formed high strength stainless steel columns. *Journal of Constructional Steel Research*, 61: 1631–49.

[38] Wang, J., Afshan, S., Gkantou, M., Theofanous, M., Baniotopoulos, C., & Gardner, L. 2016. Flexural behaviour of hot-finished high strength steel square and rectangular hollow sections. *Journal of Constructional Steel Research*, 121: 97–109.

[39] Gardner, L., Saari, N., & Wang, F. 2010. Comparative experimental study of hot-rolled and cold-formed rectangular hollow sections. *Thin-Walled Structures*, 48: 495–507.

[40] Jandera, M., Gardner, L., & Machacek, J. 2008. Residual stresses in cold-rolled stainless steel hollow sections. *Journal of Constructional Steel Research*, 64: 1255–63.

[41] Walport, F., Gardner, L., & Nethercot, D.A. 2019. A method for the treatment of second order effects in plastically-designed steel frames. *Engineering Structures*, 200: 109516.

[42] Gardner, L., Fieber, A., & Macorini, L. 2019. Formulae for calculating elastic local buckling stresses of full structural cross-sections. *Structures*, 17: 2–20.

[43] Fieber, A., Gardner, L., & Macorini, L. 2019. Formulae for determining elastic local buckling half-wavelengths of structural steel cross-sections. *Journal of Constructional Steel Research*, 159: 493–506.

[44] EN 1990. 2002. Eurocode - Basis of structural design. Brussels: CEN; 2002.

[45] Afshan, S., Francis, P., Baddoo, N.R., & Gardner, L. 2015. Reliability analysis of structural stainless steel design provisions. *Journal of Constructional Steel Research*, 114: 293–304.

[46] Tankova, T., Simões Da Silva, L., Marques, L., Rebelo, C., & Taras, A. 2014. Towards a standardized procedure for the safety assessment of stability design rules. *Journal of Constructional Steel Research*, 103: 290–302.

[47] Meng, X., Gardner, L., Sadowski, A.J., & Rotter, J.M. 2020. Elasto-plastic behaviour and design of semi-compact circular hollow sections. *Thin-Walled Structures*, 148: 106486.

[48] Yun, X., Gardner, L., & Boissonnade, N. 2018. The continuous strength method for the design of hot-rolled steel cross-sections. *Engineering Structures*, 157: 179–91.

[49] SAFEBRICTILE. 2016. Standardization of safety assessment procedures across brittle to ductile failure modes. *Grant Agreement Number: RFSR-CT-2013-00023, Deliverable D11 - Guideline for the Safety Assessment of Design Rules for Steel Structures in Line with EN 1990*,.

[50] HOLLOSSTAB. 2019. Overall-slenderness based direct design for strength and stability of innovative hollow sections. *Grant Agreement Number: RFCS-2015-709892 Deliverable D72 - Reliability Analysis of the Design Proposals and Determination of Partial Factors*,.

[51] Wang, J., & Gardner, L. 2017. Flexural buckling of hot-finished high-strength steel SHS and RHS columns. *Journal of Structural Engineering, ASCE*, 143: 1–12.

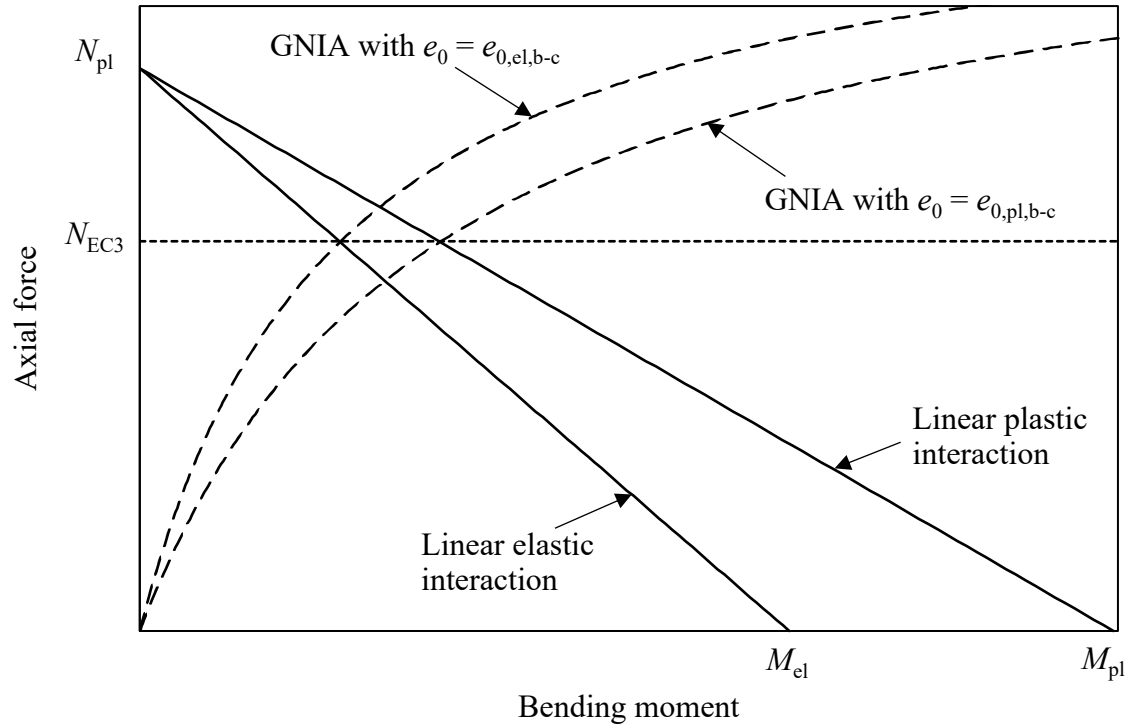

Figure 1: Cross-section interaction diagram illustrating the back-calculated equivalent imperfections included in EN 1993-1-1 and prEN 1993-1-1; use of these imperfections in a second order elastic analysis (GNIA) in conjunction with a linear M–N cross-section check results in a buckling resistance equal to that given by the Eurocode buckling curves.

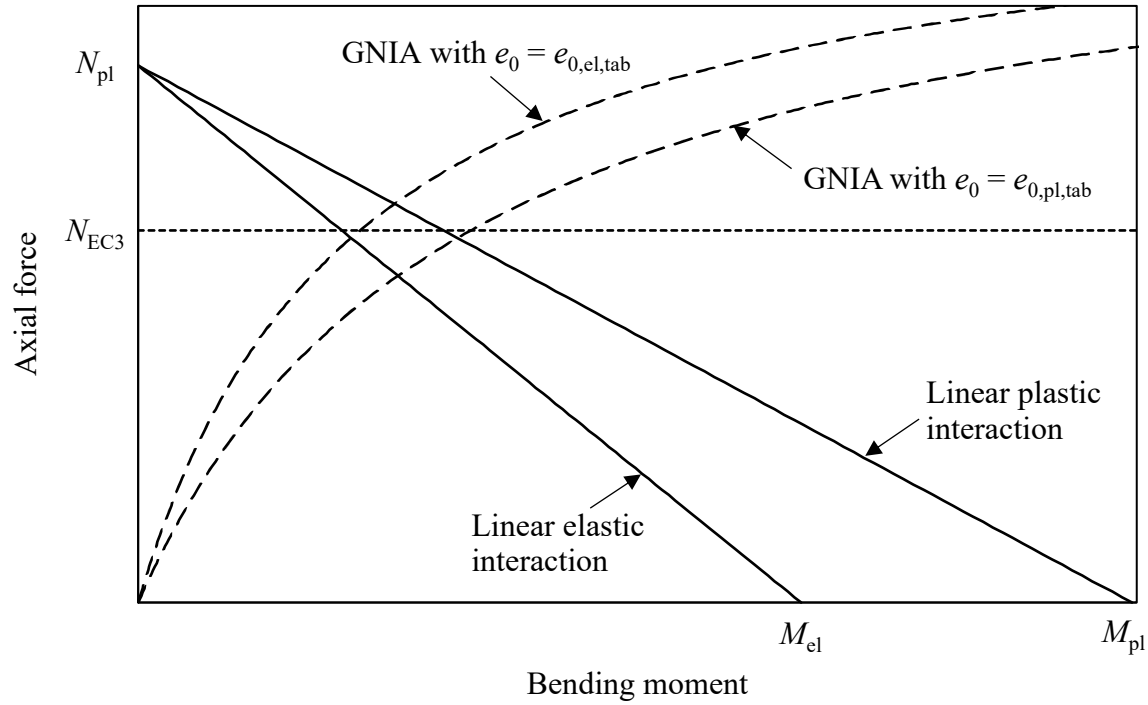

Figure 2: Cross-section interaction diagram illustrating the tabulated equivalent imperfections included in EN 1993-1-1 and prEN 1993-1-1; use of these imperfections in a second order elastic analysis (GNIA) in conjunction with a linear M–N cross-section check results in a buckling resistance (defined as the point at which the GNIA curve meets the M–N interaction line) that is close to, but on the safe-side of that given by the Eurocode buckling curves.

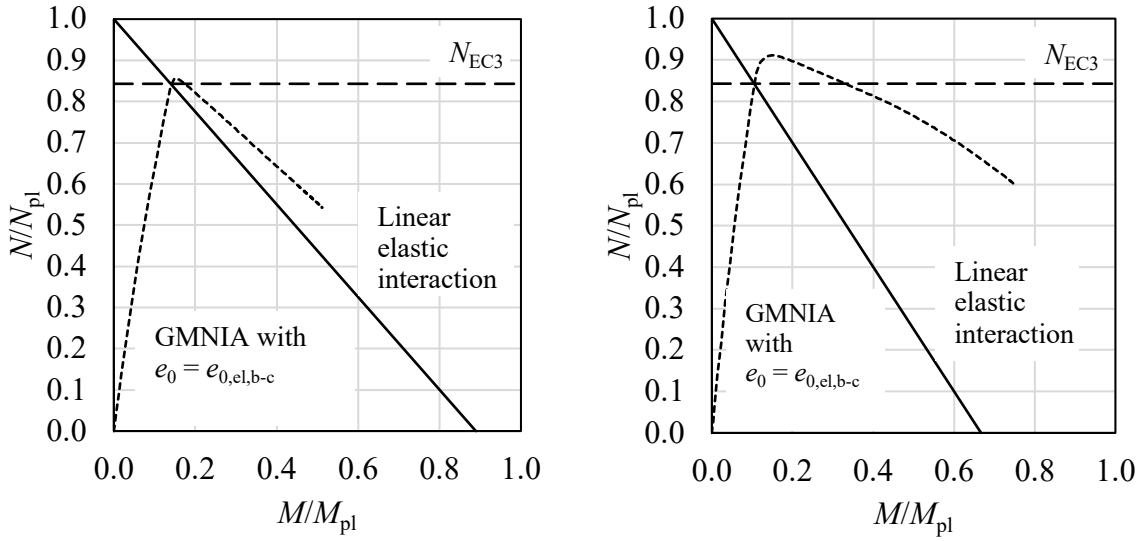

a. Major axis buckling b. Minor axis buckling

Figure 3: Over-prediction of buckling resistance when prEN 1993-1-1 equivalent back-calculated elastic imperfections are used in a second order inelastic (plastic zone) analysis (GMNIA) with a bilinear (elastic, perfectly plastic) σ–ε curve due to the post first-yielding capacity.

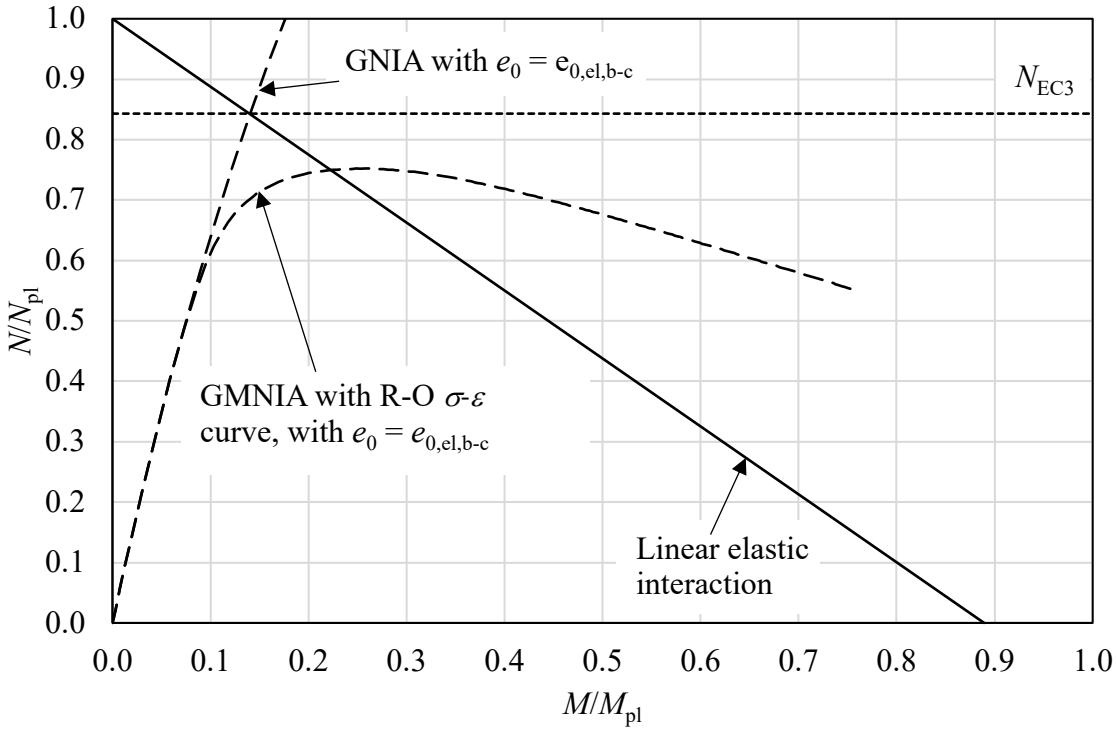

Figure 4: Under-prediction of buckling resistance when prEN 1993-1-1 equivalent back-calculated elastic imperfections are used with in a second order inelastic (plastic zone) analysis with a Ramberg–Osgood σ–ε curve due to the early material yielding.

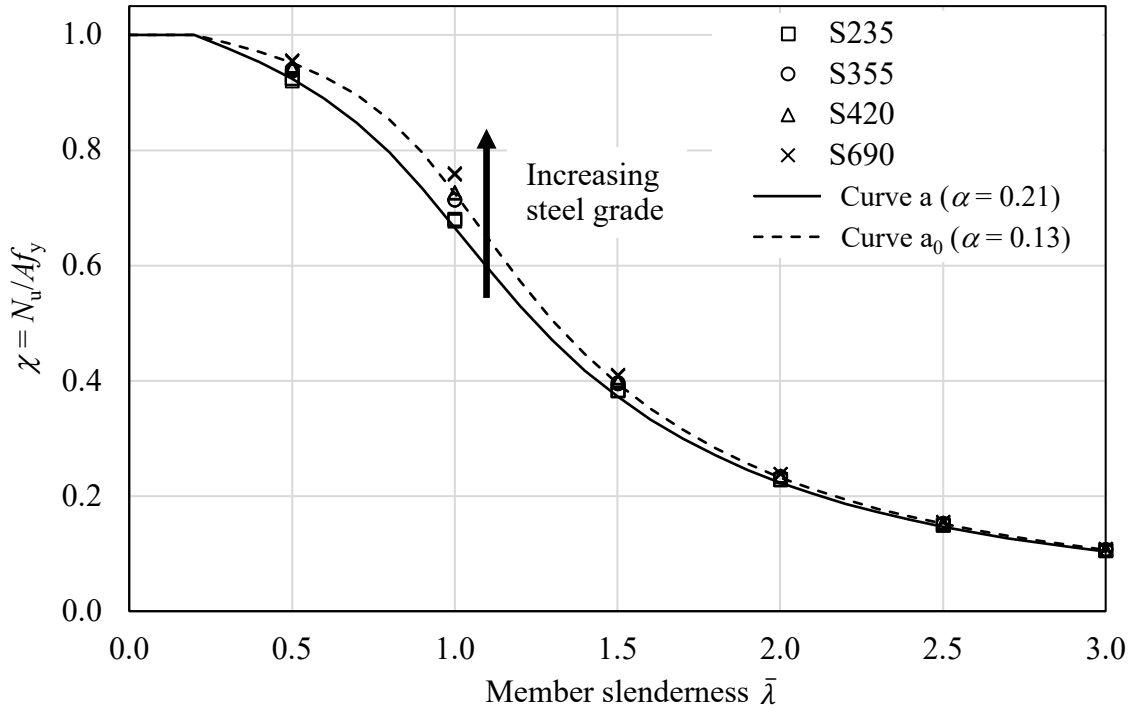

Figure 5: Variation of buckling capacity with steel grade; individual buckling curves become increasingly conservative with increasing yield stress.

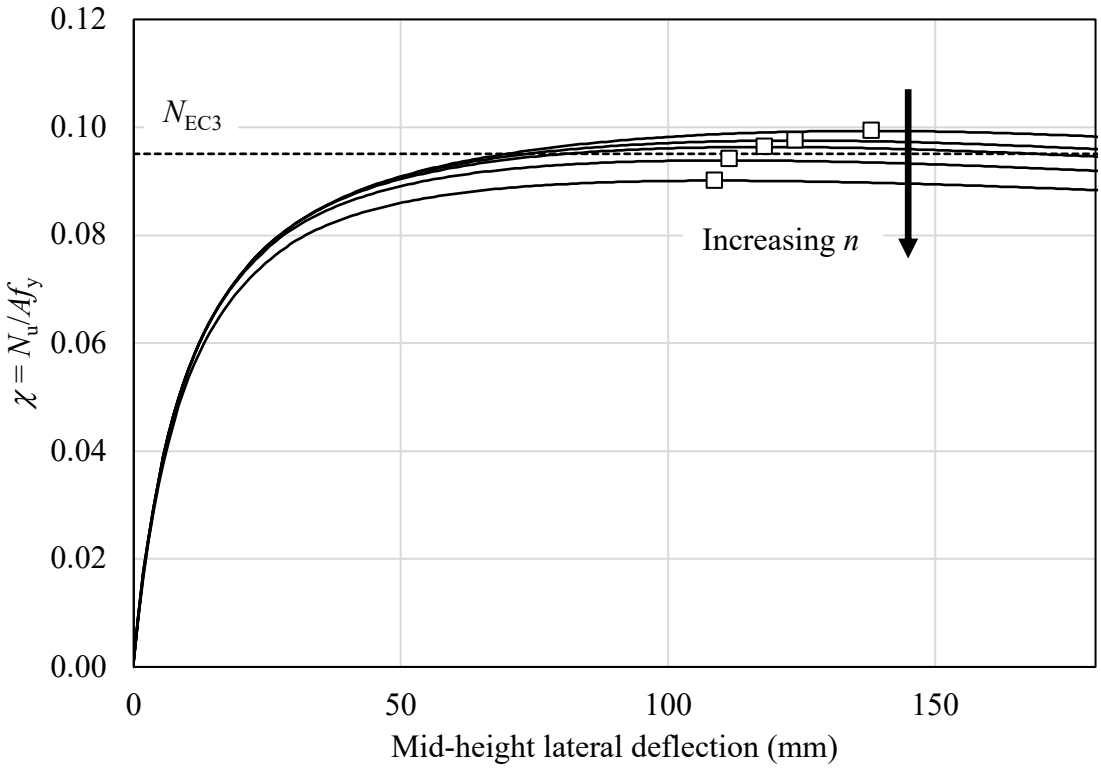

Figure 6: Variation of buckling capacity with varying Ramberg–Osgood exponent n; increasing n values result in lower buckling capacity, though this effect is not captured by individual buckling curves.

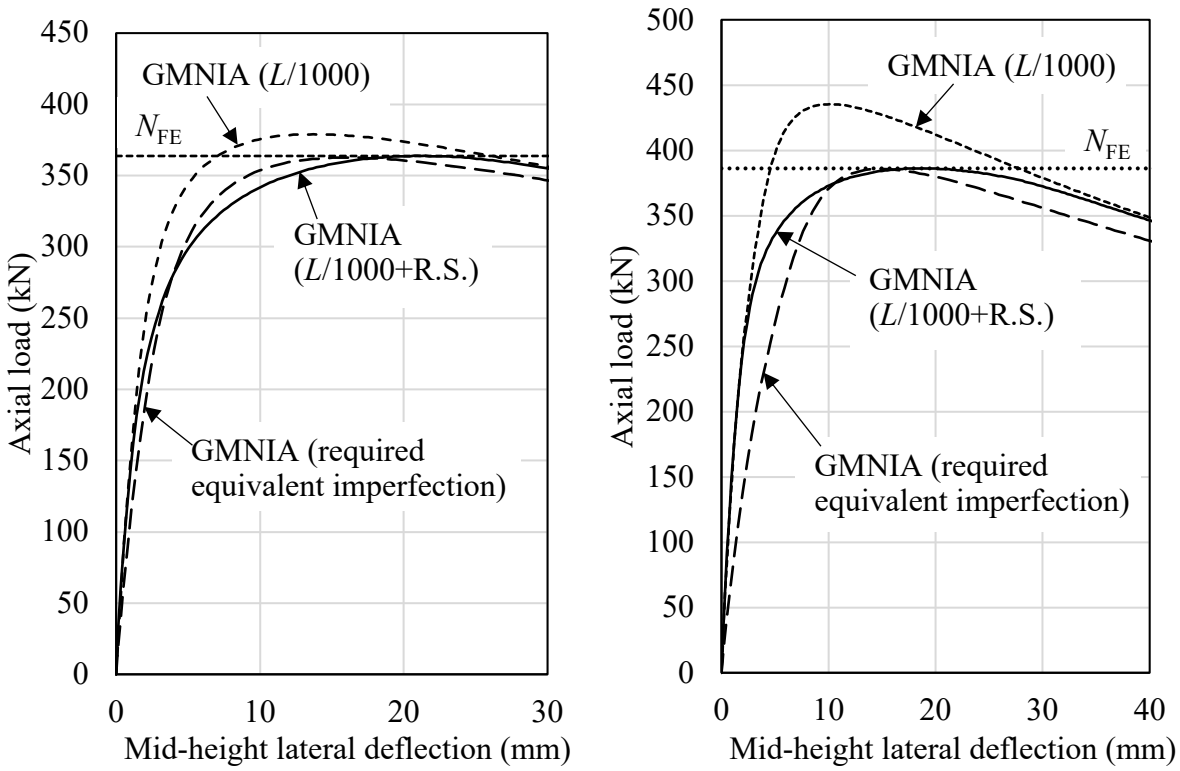

Figure 7: Required equivalent imperfections calculated to within 1% of the benchmark FE ultimate loads N_{FE} as calculated using GMNIA with imperfection magnitudes of $L/1000$ and residual stresses (R.S.).

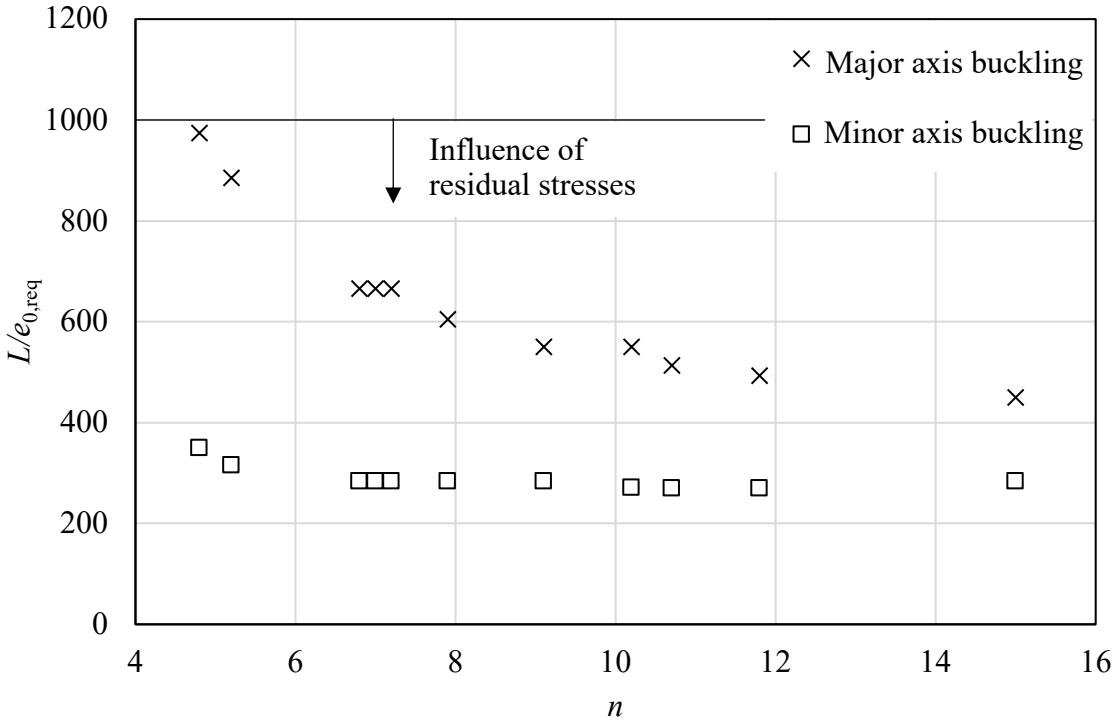

Figure 8: Increasing influence of residual stresses from major axis buckling to minor axis buckling, as well as with increasing strain hardening exponent n (i.e. residual stresses have a reduced influence the more rounded the material stress–strain response).

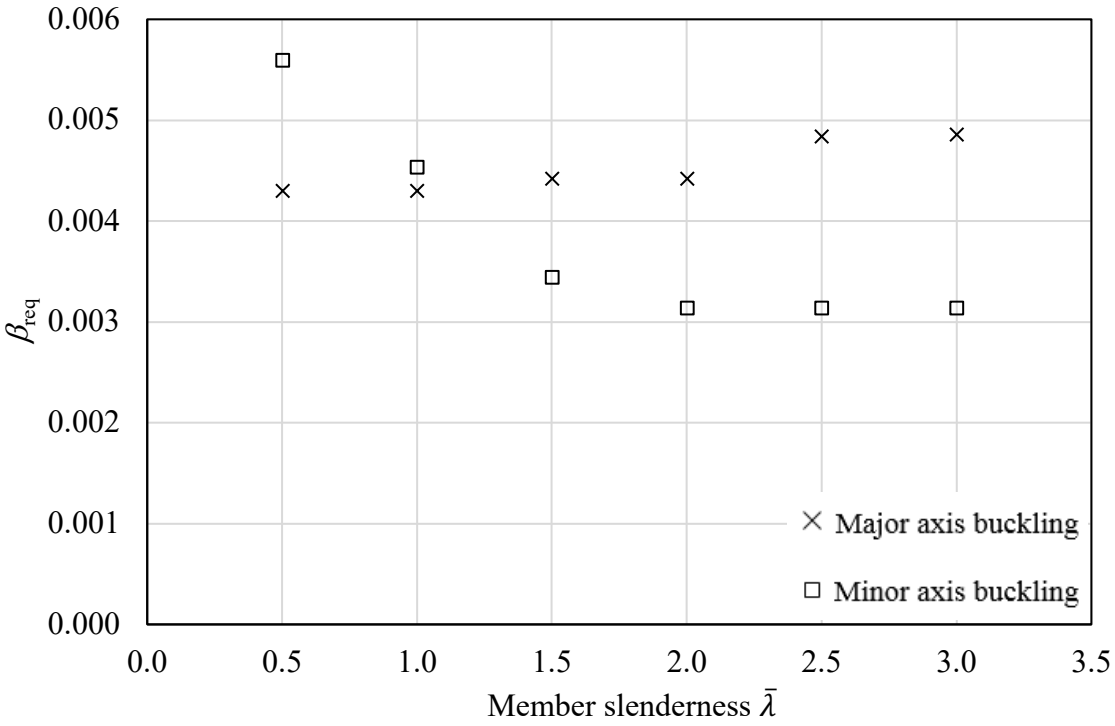

Figure 9: Required reference relative bow imperfection β_{req} values for an example hot-rolled steel I-section with varying member slenderness buckling about the major and minor axes.

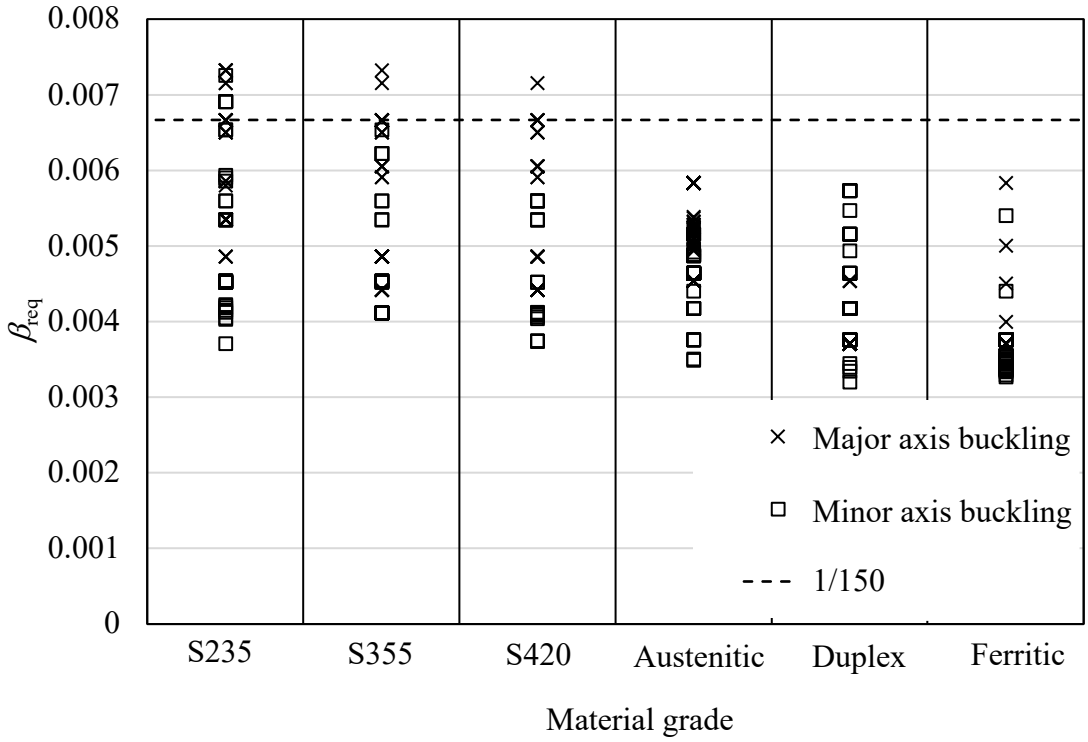

Figure 10: Required reference bow imperfection β_{req} values for I-sections, for all considered materials and both axes of buckling.

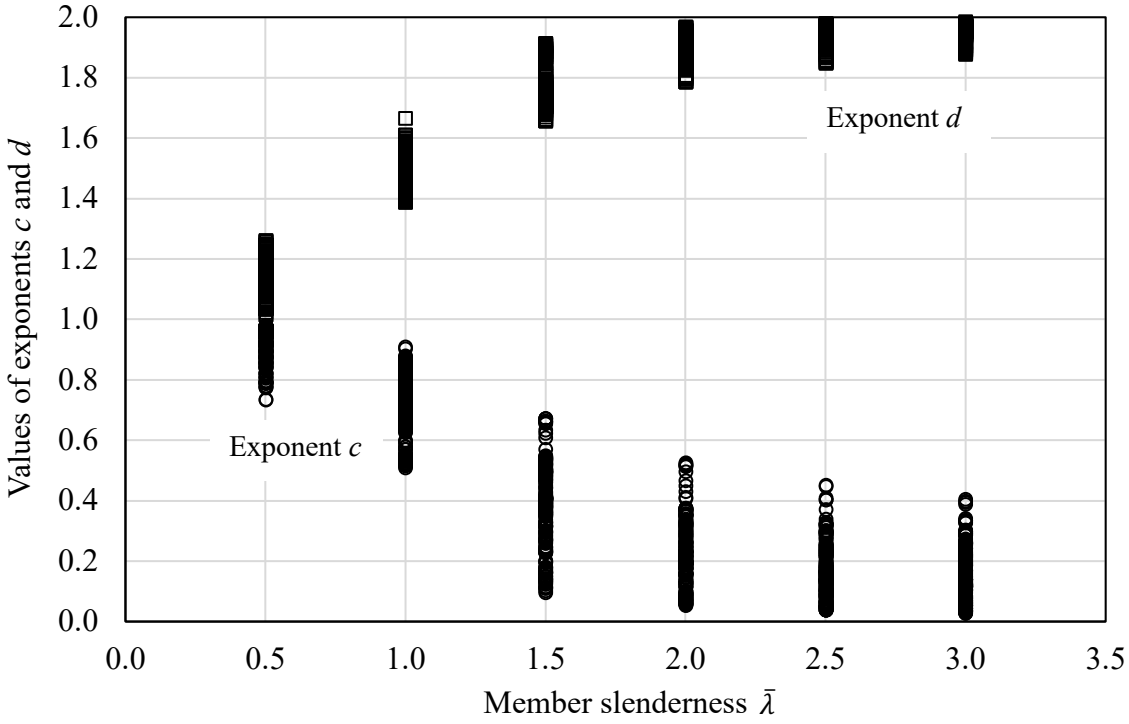

Figure 11: Values of the exponents c and d reflecting the dependency of the buckling resistance on the yield stress f_y and cross-section area A, respectively, for all cases considered.

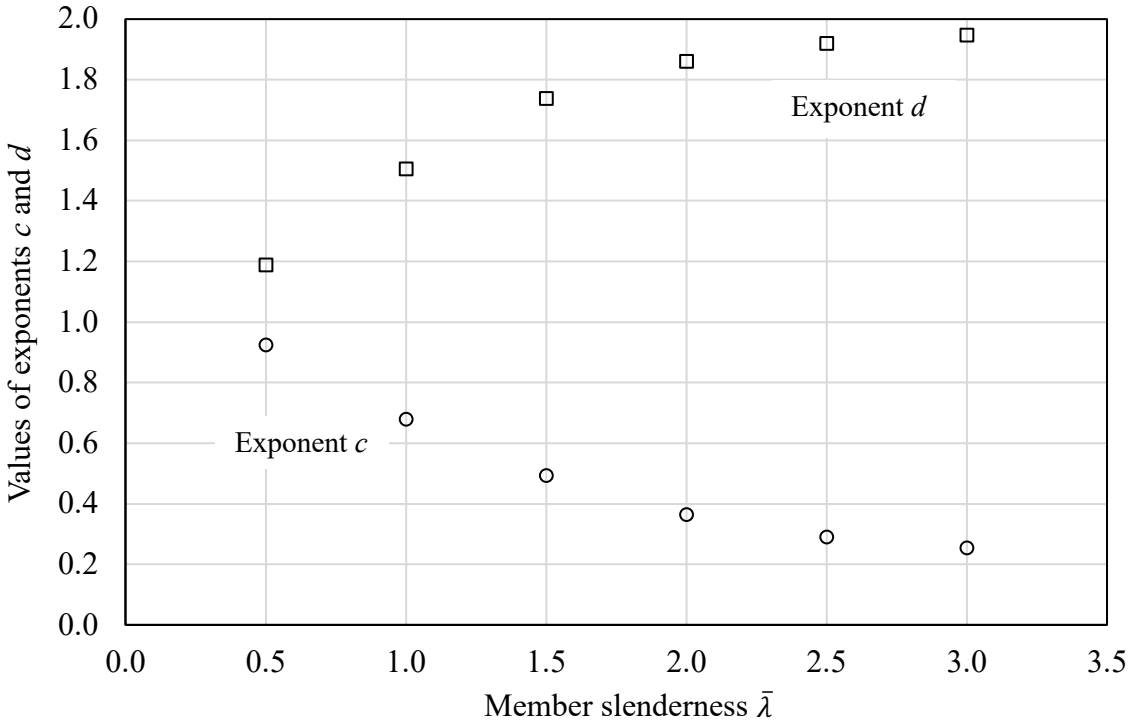

Figure 12 : Values of exponents c and d reflecting the dependency of the buckling resistance on the yield stress f_y and cross-section area A, respectively, for a hot-rolled S235 steel HEB 100 cross-section buckling about the major axis.

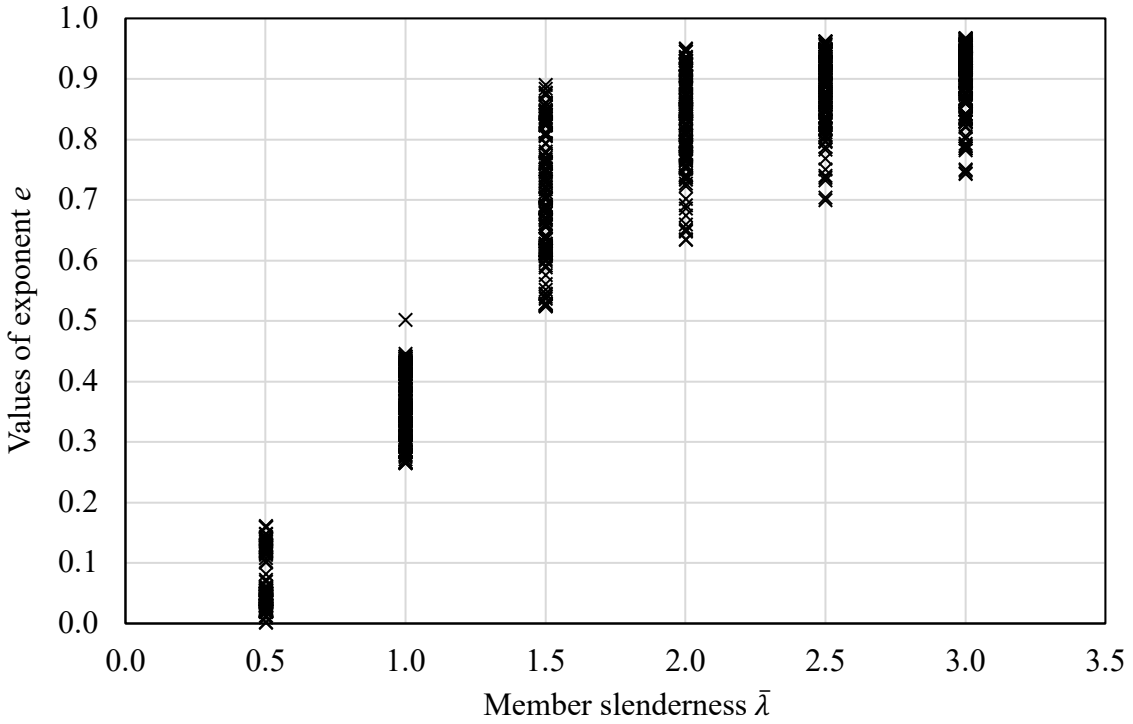

Figure 13: Values of exponent e reflecting the dependency of the buckling resistance on the Young's modulus E for all cases considered.

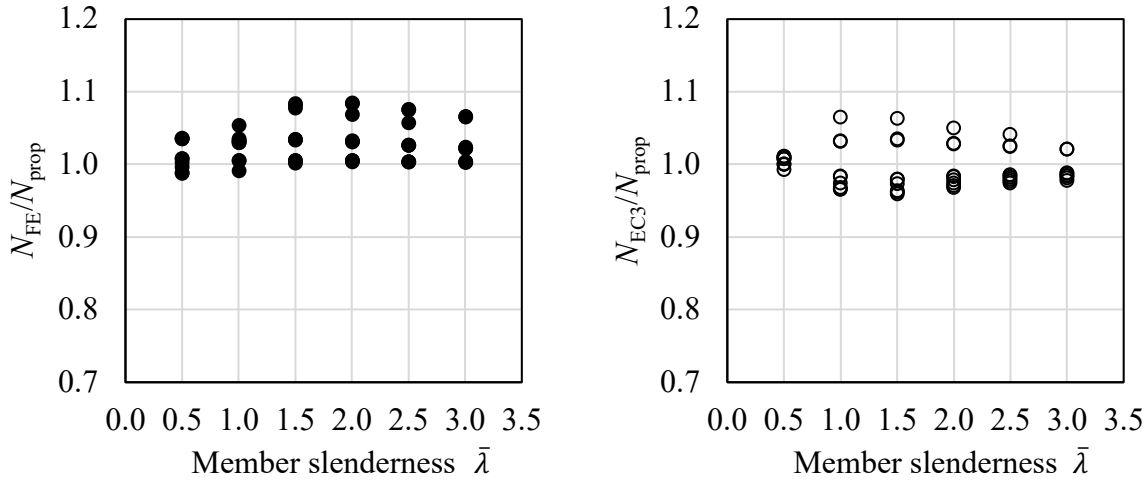

a. S235

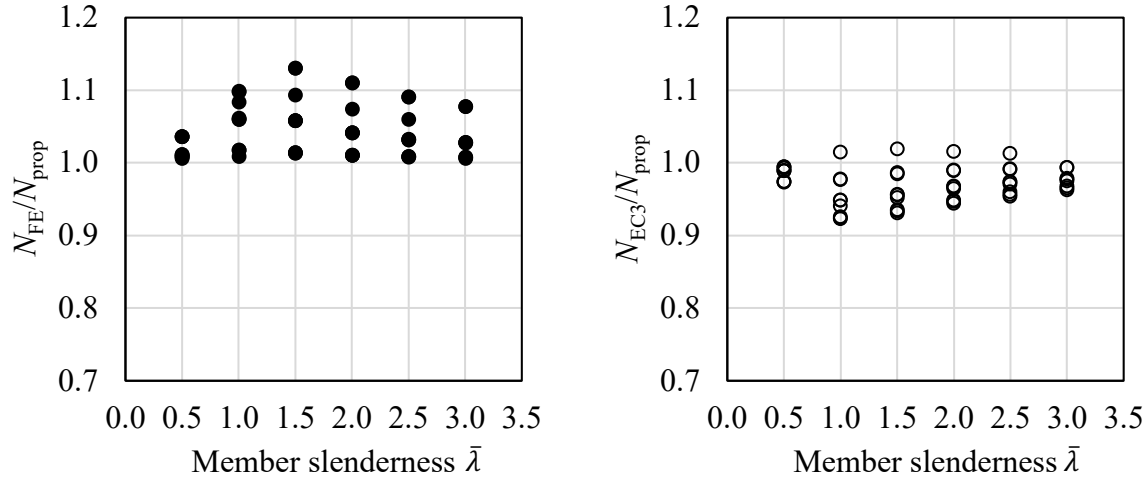

b. S355

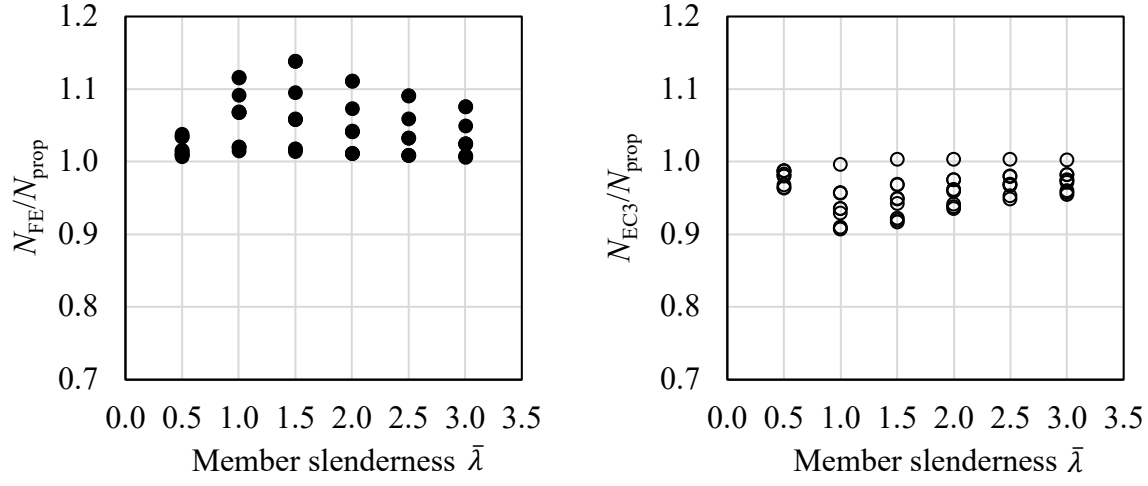

c. S420

Figure 14: Comparisons of the resistance predictions obtained using the proposed method of design by second order inelastic analysis N_{prop}, the benchmark FE models N_{FE}, and the prEN 1993-1-1 buckling curves N_{EC3}.

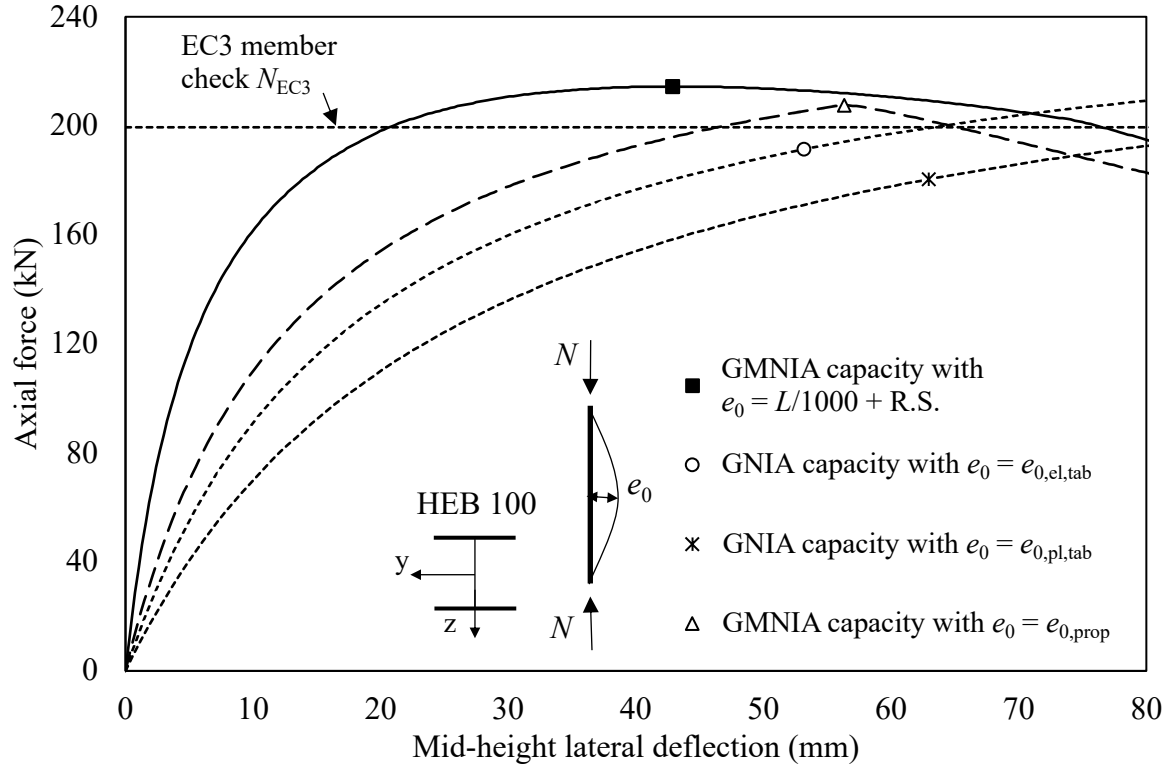

Figure 15: Load–deformation paths and ultimate resistance predictions (indicated by the position of the symbols) for a hot-rolled S235 steel HEB 100 column buckling about the major axis with $\bar{\lambda} = 1.5$ for a range of analysis/design approaches.

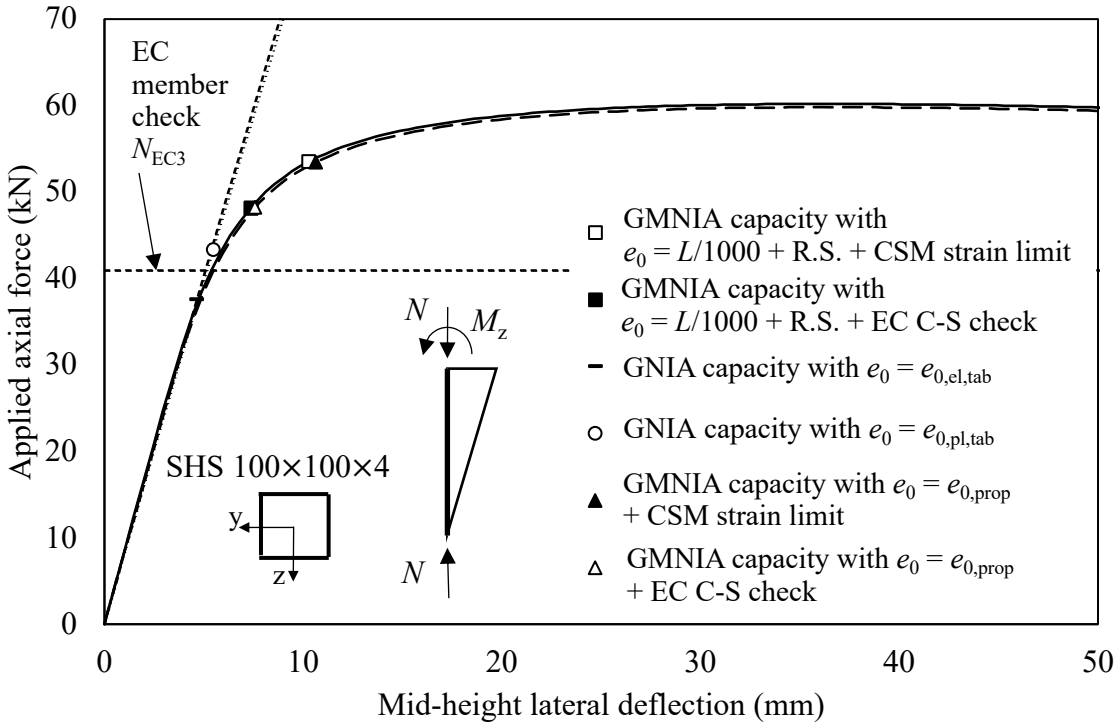

Figure 16: Load–deformation paths and ultimate resistance predictions (indicated by the position of the symbols) for an austenitic ($n = 7$) stainless steel SHS 100 × 100 × 4 beam-column with $\bar{\lambda} = 0.5$ for a range of analysis/design approaches.

Table 1: Material model parameters used for comparative parametric studies

	Young's modulus E (N/mm^2)	Yield (0.2% proof) stress f_y (N/mm^2)	Ultimate stress f_u (N/mm^2)	Ultimate strain ε_u	Strain hardening strain ε_{sh}	Strain hardening exponent n	Strain hardening exponent m
Hot-rolled steel	210,000	235	360	0.21	0.015	-	-
		355	490	0.17	0.017		
		420	540	0.13	0.023		
High-strength steel	210,000	690	770	0.06	0.035	-	-
Cold-formed (C-F) steel	210,000	355	490	0.17	-	8	3.8
Austenitic (A) stainless steel	200,000	280	580	0.50	-	5.2, 6.8, 7, 7.2, 7.9, 9.1, 10.2, 10.7, 11.8, 15	2.3
Duplex (D) stainless steel	200,000	530	770	0.30	-	4.5, 6.9, 7.2, 7.9, 8, 8.1, 8.3, 9.3, 9.6, 10.6, 13	3.6
Ferritic (F) stainless steel	200,000	320	480	0.16	-	9.8, 11.8, 13.5, 14, 15.5, 16.9, 17.2, 17.4, 17.8, 18.5, 21.6	2.8

Table 2: Summary of the statistical analysis results for the proposed approach applied to I-section columns of varying slenderness ($\bar{\lambda}$ = 0.5, 1.0, 1.5, 2.0, 2.5, 3.0) buckling about the major and minor axes assessed against the benchmark FE results

Material	Grade	No.	$f_{y,mean}/f_{y,nom}$	V_{fy}	V_A	V_E	b	V_δ	γ_{M1}
Steel	235	54	1.25	0.055	0.022	0.03	1.03	0.03	1.04
	355	54	1.20	0.050	0.022	0.03	1.04	0.03	1.05
	420	54	1.20	0.050	0.022	0.03	1.05	0.04	1.05
Stainless steel	A	308	1.30	0.060	0.022	0.03	1.09	0.04	0.98
	D	308	1.10	0.030	0.022	0.03	1.11	0.03	1.02
	F	308	1.20	0.045	0.022	0.03	1.12	0.05	0.98

Table 3: Summary of the statistical analysis results for the proposed approach applied to hollow section columns of varying slenderness ($\bar{\lambda}$ = 0.5, 1.0, 1.5, 2.0, 2.5, 3.0) buckling about the major and minor axes assessed against the benchmark FE results

Material	Grade	No.	$f_{y,mean}/f_{y,nom}$	V_{fy}	V_A	V_E	b	V_δ	γ_{M1}
Steel	235	36	1.25	0.055	0.027	0.03	1.03	0.01	1.05
	355	36	1.20	0.050	0.027	0.03	1.03	0.01	1.05
	420	36	1.20	0.050	0.027	0.03	1.02	0.01	1.05
High-strength steel	690	36	1.10	0.035	0.027	0.03	0.99	0.00	1.10
Cold-formed steel	355	36	1.20	0.045	0.027	0.03	1.15	0.04	0.97
Stainless steel	A	66	1.30	0.060	0.027	0.03	1.16	0.04	0.94
	D	66	1.10	0.030	0.027	0.03	1.13	0.04	1.01
	F	66	1.20	0.045	0.027	0.03	1.09	0.03	0.99

Table 4: Summary of the statistical analysis results for the proposed approach applied to I-section beam-columns of varying slenderness ($\bar{\lambda} = 0.5, 1.0, 1.5$) buckling about the major and minor axes assessed against the benchmark FE results

Material	Grade	No.	$f_{y,mean}/f_{y,nom}$	V_{fy}	V_A	V_E	b	V_δ	γ_{M1}
Steel	235	36	1.25	0.055	0.022	0.03	1.02	0.01	0.95
	355	36	1.20	0.050	0.022	0.03	1.01	0.01	0.99
	420	36	1.20	0.050	0.022	0.03	1.04	0.02	0.96
Stainless steel	A	36	1.30	0.060	0.022	0.03	1.04	0.02	0.95
	D	36	1.10	0.030	0.022	0.03	1.05	0.03	1.05
	F	36	1.20	0.045	0.022	0.03	1.04	0.03	1.01

Table 5: Summary of the statistical analysis results for the proposed approach applied to hollow section beam-columns of varying slenderness ($\bar{\lambda} = 0.5, 1.0, 1.5$) buckling about the major and minor axes assessed against the benchmark FE results

Material	Grade	No.	$f_{y,mean}/f_{y,nom}$	V_{fy}	V_A	V_E	b	V_δ	γ_{M1}
Steel	235	52	1.25	0.055	0.027	0.03	1.02	0.01	0.97
	355	52	1.20	0.050	0.027	0.03	1.01	0.01	1.01
	420	52	1.20	0.050	0.027	0.03	1.01	0.01	1.02
High-strength steel	690	52	1.10	0.035	0.027	0.03	1.00	0.00	1.06
Cold-formed steel	355	52	1.20	0.045	0.027	0.03	1.06	0.03	1.00
Stainless steel	A	36	1.30	0.060	0.027	0.03	1.08	0.05	0.96
	D	36	1.10	0.030	0.027	0.03	1.06	0.04	1.06
	F	36	1.20	0.045	0.027	0.03	1.07	0.04	0.99

Table 6: Summary of comparisons between benchmark FE resistance N_{FE} and that defined using the range of considered design methods N_{e0} for the two worked examples; all models utilised the linear Timoshenko B31 beam element.

Imperfection e_0	Analysis type	Cross-section resistance	Worked example 1 – S235 steel HEB 100 I-section ($L_{b,cs}$ = 170 mm, $\bar{\lambda}_p$ = 0.27) column buckling about major axis N_{FE}/N_{e0}	Worked example 2 – austenitic stainless steel (f_y = 280 N/mm^2, n = 7) stainless steel SHS 100×4 ($L_{b,cs}$ = 84 mm, $\bar{\lambda}_p$ = 0.42) beam-column N_{FE}/N_{e0}
Benchmark $L/1000$ + R.S.	Plastic zone	CSM strain limit	1.00	1.00
		EC nonlinear plastic M-N check		0.90
$e_{0,el,tab}$	Elastic	EC linear elastic M-N check	0.89	0.70
$e_{0,pl,tab}$	Elastic	EC linear plastic M-N check	0.84	0.81
$e_{0,el,tab}$	Plastic zone	CSM strain limit	0.91	0.99
		EC nonlinear plastic M-N check		0.90
$e_{0,pl,tab}$	Plastic zone	CSM strain limit	0.83	0.99
		EC nonlinear plastic M-N check		0.90
$e_{0,prop}$ (Eq. (21))	Plastic zone	CSM strain limit	0.97	1.00
		EC nonlinear plastic M-N check		0.90